CHAPTER 11

CRYOGENICS

11.1 OVERVIEW

The LHC is unique among superconducting synchrotrons [1, 2, 3] because its operating temperature is below 2 K in order to maximise the field strength of the superconducting magnets with NbTi windings. The evolution of the basic design criteria and constraints as well as the main technical choices for the LHC cryogenic system are described in Chapter 6 of the 'Pink Book' [4], in Part III, Section 2 of the 'White Book' [5] and in Part III, Section 2 of the 'Yellow Book' [6]. This chapter describes the design of the LHC cryogenic system as it stands in 2004.

11.2 FUNCTIONS, CONSTRAINTS, ARCHITECTURE

11.2.1 General Functions

The superconducting magnet windings in arcs, dispersion suppressors and inner triplets will be immersed in a pressurised bath of superfluid helium at about 0.13 MPa (1.3 bar) and a maximum temperature of 1.9 K [7, 8]. This allows a sufficient temperature margin for heat transfer across the electrical insulation. As the specific heat of the superconducting alloy and its copper matrix fall rapidly with decreasing temperature, the full benefit in terms of stability margin of operation at 1.9 K instead of at the conventional 4.5 K may only be reaped by making effective use of the transport properties of superfluid helium, for which the temperature of 1.9 K also corresponds to a maximum in the effective thermal conductivity [9]. The low bulk viscosity enables the coolant to permeate the heart of the magnet windings, while the very large specific heat (typically 10^5 times that of the conductor per unit mass, 2×10^3 times per unit volume), combined with the enormous heat conductivity at moderate flux (3000 times that of cryogenic-grade OFHC copper, peaking at 1.9 K) can have a powerful stabilising action on thermal disturbances. To achieve this, the electrical insulation of the conductor must preserve sufficient porosity and thermal percolation paths while still fulfilling its demanding dielectric and mechanical duties. This cooling requirement applies during both ramping and stored-beam operation. In the case of fast current discharge, the temperature excursion may be larger but must still remain below the helium II/helium I phase transition (lambda line). In the long straight sections, with the exception of the inner triplets and the superconducting dipoles D1, the field strength and heat extraction requirements are such that operation at 1.9 K is not necessary. These magnets will have their superconducting windings immersed in a bath of saturated helium at a temperature of 4.5 K.

The cryogenic system [10, 11] must cope with load variations and large dynamic range induced by operation of the accelerator.

The LHC cryogenic system must also be able to cool-down and fill the huge cold mass of the LHC, 37×10^6 kg in a maximum time of 15 days while avoiding thermal gradients in the cryo-magnet structure higher than 75 K. This limit in thermal gradient and time also applies to the forced emptying and warm-up of the machine prior to shutdown periods.

The cryogenic system must be able to cope with the resistive transitions of the superconducting magnets, which occasionally will occur in the machine, while minimising loss of cryogen and system perturbations. It must handle the resulting heat release and its consequences, which include fast pressure rises and flow surges. It must limit the propagation to the neighbouring magnets and recover in a time that does not seriously detract from the operational availability of the LHC. A resistive transition extending over one lattice cell should not result in a down time of more than a few hours.

In addition to these basic operational duties, the LHC cryogenic system should allow for rapid cool-down and warm-up of limited lengths of cryo-magnet strings, e.g. for repairing or exchanging a defective unit. It should also be able to cope with the resistive transition of a full sector - this defining the maximum credible

incident - without impairing personnel or equipment safety. Finally, to ensure reliable operation, it should provide some redundancy among its components and sub-systems.

11.2.2 Design Constraints

The main constraints result from the need to install the system in the existing LEP tunnel and re-use its facilities, including the four existing LEP refrigerators [12] and their cryogenic infrastructure. The limited number of access points to the underground areas is reflected in the architecture of the LHC cryogenic system. The cooling power required at each temperature level will be produced in eight refrigeration plants and distributed to the adjacent sectors over distances of up to 3.3 km. For reasons of simplicity, reliability and maintenance, the number of active cryogenic components distributed around the ring is minimised.

To simplify the magnet string design, the cryogenic headers distributing the cooling power along a machine sector as well as all remaining active cryogenic components in the tunnel are contained in a compound cryogenic distribution line (QRL). The QRL runs alongside the cryo-magnet strings in the tunnel and feeds each 106.9 m-long lattice cell in parallel via a jumper connection (Fig. 11.1). Choosing spacing of the jumper connections to be one full cell length was the result of an optimisation exercise [13].

The LHC tunnel is inclined at 1.41 % with respect to the horizontal, thus giving rise to elevation differences of up to 120 m across the tunnel diameter. This will generate hydrostatic heads in the cryogenic headers and could generate flow instabilities in two-phase, liquid-vapour, flow. To avoid these harmful instabilities, all fluids should ideally be transported over large distances in mono-phase state, i.e. in the superheated-vapour or supercritical region of the phase diagram. Local two-phase circulation of saturated liquid can be tolerated over limited lengths, in a controlled direction of circulation.

Equipment is installed as much as possible above ground to avoid the need for excavation of further large underground caverns. However, certain components which must be close to the cryostats or which cannot be installed on the surface because of the hydrostatic head will be installed underground.

For reasons of safety the use of nitrogen in the tunnel is forbidden and discharge of helium is restricted to small quantities only. These safety aspects are reflected in specific operational design features of the system, such as the inclusion of a large acceptance cold recovery header inside the QRL.

The cryogenic system is designed for fully automatic operation during nine consecutive months followed by three months of shutdown during which maintenance will be performed.

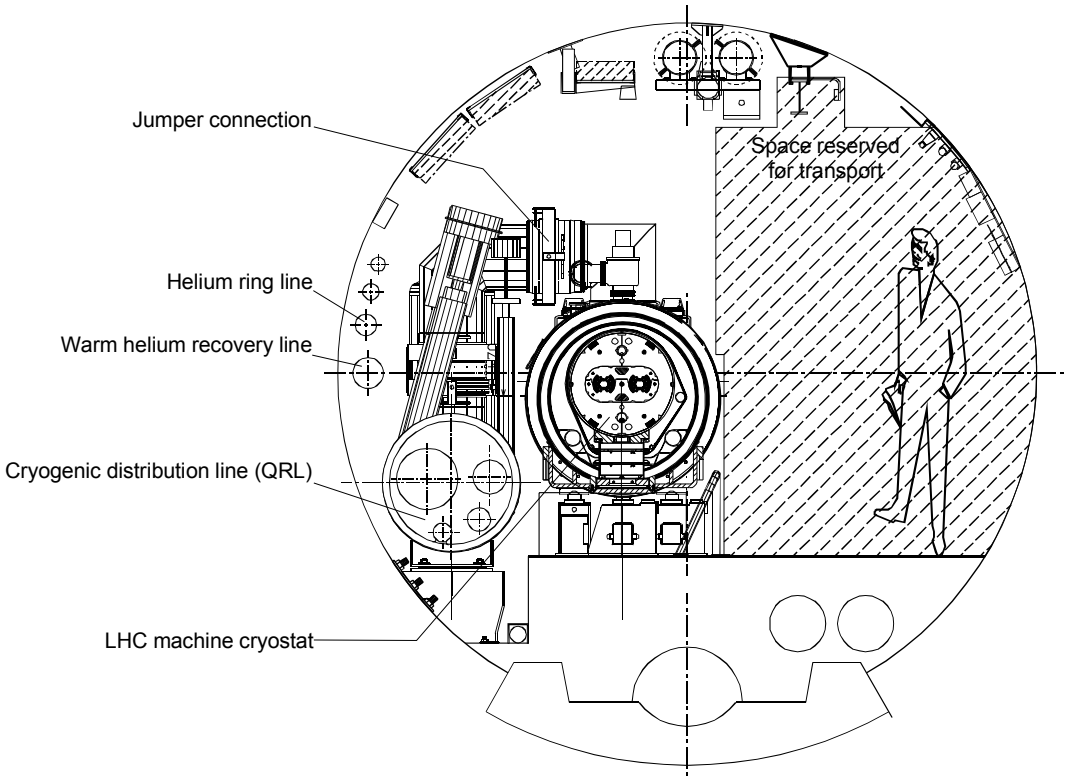

Figure 11.1: Transverse cross-section of the LHC tunnel

11.2.3 General Architecture

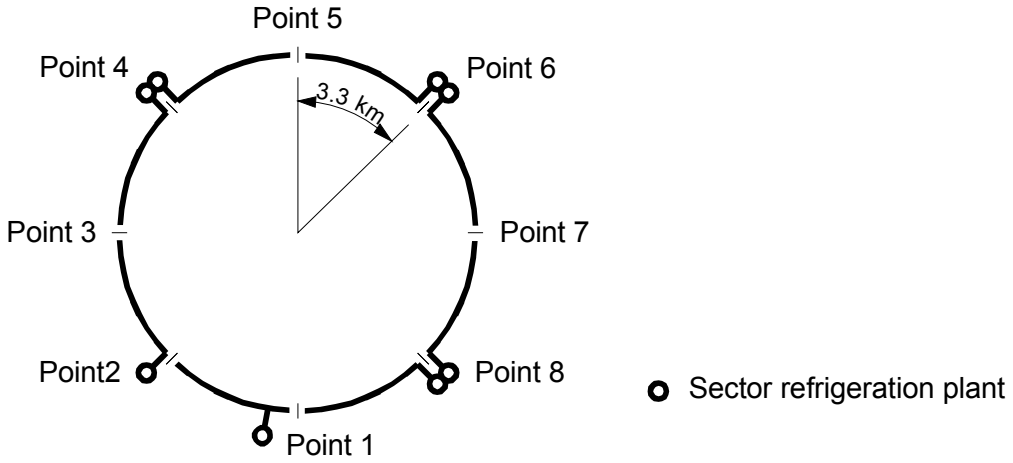

Figure 11.2: General layout of the cryogenic system

A direct consequence of the site constraints is the cryogenic layout of the machine (Fig. 11.2), with five cryogenic "islands" at access points 1.8, 2, 4, 6 and 8 where all refrigeration and ancillary equipment is concentrated. Equipment at ground level includes electrical substation, warm compressor station (QCS_A,B,C), cryogen storage (helium and liquid nitrogen), cooling towers, cold-boxes (QSR_A,B) and underground are the lower cold-boxes (QURA), 1.8 K refrigeration unit boxes (QURC), interconnecting lines, and interconnection boxes (QUI_A,B,C). Each cryogenic island houses one or two refrigeration plants that feed one or two adjacent tunnel sectors, requiring distribution and recovery of the cooling fluids over distances of 3.3 km underground. Fig. 11.3 shows the general architecture of the cryogenic system. A refrigeration plant comprises one 4.5 K refrigerator and one 1.8 K refrigeration unit. The 4.5 K refrigerator is either one of the four split-cold-box refrigerators recovered from LEP or one of the four new integrated-cold-box refrigerators. At each cryogenic island, an interconnection box couples the various refrigeration equipments and the cryogenic distribution line. They also permit, when possible, redundancy in between the refrigeration plants.

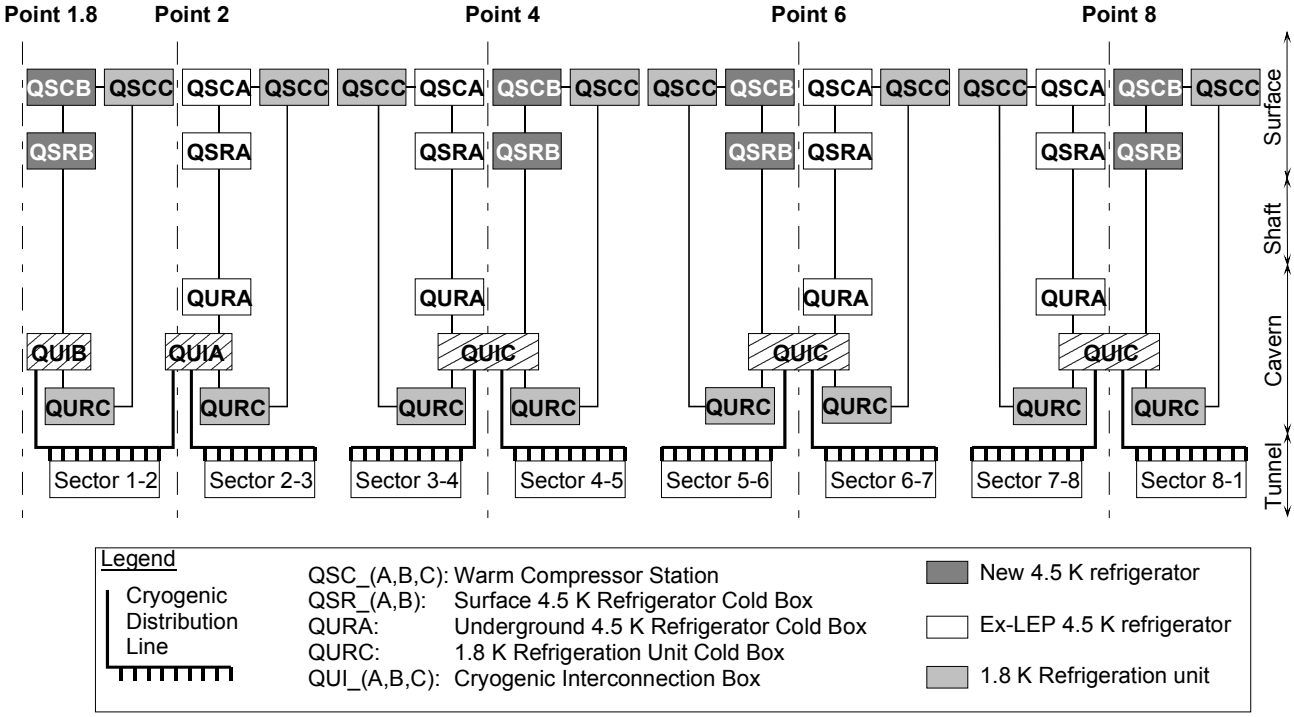

Figure 11.3: General architecture of the cryogenic system

Due to the lack of space for two refrigeration plants at Point 2 and the need at Point 1.8 for large refrigeration capacity for cryo-magnet testing, the 4-point symmetry was broken and two refrigeration plants at points 4, 6 and 8 and only one refrigeration plant at points 1.8 and 2 were installed. The drawback of this architecture concerns sector 2-3, which only benefits from limited redundancy.

To limit the environmental impact as well as the pressure build-up during helium discharge in the case of quench of a magnet sector, helium storage is provided at all eight access points.

11.3 TEMPERATURE LEVELS

In view of the high thermodynamic cost of refrigeration at 1.8 K, the thermal design of the LHC cryogenic components aims at intercepting the largest fraction of applied heat loads at higher temperature, hence the multiple, staged temperature levels in the system. The temperature levels are:

- 50 K to 75 K for thermal shield as a first major heat intercept, sheltering the cold mass from the bulk of heat in-leaks from ambient.
- 4.6 K to 20 K for lower temperature heat interception and for the cooling of the beam screens which protect the magnet cold bore from beam-induced loads.
- 1.9 K quasi-isothermal superfluid helium for cooling the magnet cold mass.
- 4 K at very low pressure (VLP) for transporting the superheated helium flow coming from the distributed 1.8 K heat exchanger tubes across the sector length to the 1.8 K refrigeration units.
- 4.5 K normal saturated helium for cooling special superconducting magnets in insertion regions, superconducting acceleration cavities, and the lower sections of high temperature superconductor (HTS) current leads.
- 20 K to 300 K cooling for the resistive upper sections of HTS current leads [14].

To provide cooling at these temperature levels, the LHC cryogenic system makes use of helium in several thermodynamic states, shown in Fig. 11.4 on a pressure-temperature phase diagram.

The cryostats [15] (see Chap. 7) and cryogenic distribution line [16] combine several low-temperature insulation and heat interception techniques, which will have to be reliably implemented on an industrial scale. These include low-conduction support posts made of non-metallic glass-fibre/epoxy composite [17], low-impedance thermal contacts under vacuum for heat intercepts and multi-layer reflective insulation wrapping the some 80,000 m^2 of cold surface area below 20 K [18]. Each of these techniques was investigated and validated separately in the laboratory [19], and the complete cryostats were then modelled by thermal network analysis and optimised in standard as well as off-design operation [20]. Precision experimental measurements confirmed the soundness of the adopted design and its suitability for industrial construction [21].

Besides their primary function of intercepting beam-induced heat loads at a temperature well above that of the magnets, the beam screens also act as an intermediate-temperature baffle for the cryo-pump constituted by the 1.9 K surface of the magnet bores, thus sheltering the cold surface from synchrotron radiation, preventing desorption of the trapped gas molecules and avoiding breakdown of the beam vacuum [22] (see Chap. 12). In order to limit resistive heating as well as residual heat in-leaks to the magnets, the beam screens must operate below about 30 K. To match the available temperature levels in the existing refrigerators, they are cooled non-isothermally by a forced flow of weakly supercritical helium, between 4.6 K and 20 K, which reduces the entropic load by a factor 8 with respect to 1.9 K isothermal refrigeration. The choice of mono-phase, supercritical helium aims at avoiding the potential problems of two-phase flow in long, narrow channels. However, the strongly varying properties of helium close to the critical point may nevertheless create thermo-hydraulic instabilities, while the large aspect ratio of the cooling channels induces long control delays. These problems have been investigated both theoretically and experimentally on a full-scale test loop [23] and on prototype magnet string [24, 25], thus permitting the identification of critical parameters and the validation of the adequate steady-state and transient performance of the solution proposed [26].

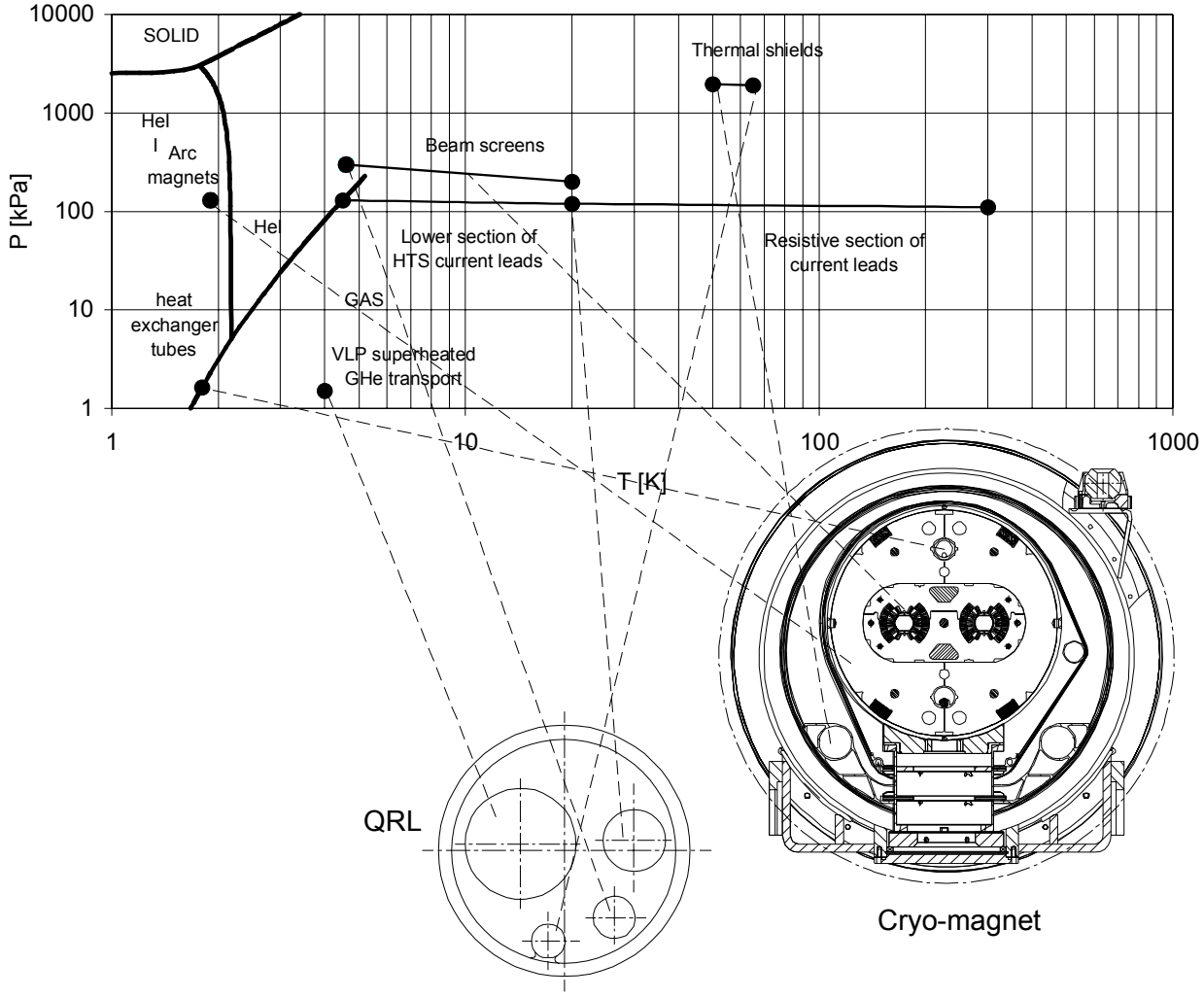

Figure 11.4 Thermodynamic states of helium in the LHC cryogenic system

11.4 HEAT LOADS

11.4.1 Steady Operation

Heat in-leaks

Static heat in-leaks are a function of the design of the cryostats and originate at the ambient temperature environment. Thermal calculations, conducted on the basis of the detailed construction drawings, precise heat in leak measurements on critical components and global measurements performed on prototype cryo-magnets, test string and a full-scale thermal model, have allowed the heat in-leaks to be evaluated. This has confirmed the technical feasibility of efficient compound cryostats [27, 28, 29, 30, 31, 32], housing long superconducting magnets operating in superfluid helium. Tab. 11.1, 2 & 3 give the steady-state heat in-leaks in standard cells, arcs, dispersion suppressors (DS), long straight sections (LSS), QRL sectors and associated distribution equipments.

Table 11.1: Distributed static heat in-leaks in a standard cell [W m^{-1}] (no contingency)

Temperature level	50-75 K	4.6-20 K	1.9 K LHe	4 K VLP GHe
Magnet side	4.5	0.14	0.19	0
QRL side	3.2	0.09	0.02	0.11

Table 11.2: Static heat in-leaks in standard cell, arc, DS and LSS (Magnet side) (no contingency)

Temperature level	50-75 K [W]	4.6-20 K [W]	4.5 K LHe [W]	1.9 K LHe [W]	20-300 K [g/s]
Cell	482	14.0	-	20.4	-
Arc (23 cells)	11090	323	-	470	-
DS 1, 2, 4, 5, 6 & 8 *	788	28	0	34	-
DS 3 & 7 *	794	28	0	34	-
LSS 1 & 5 *	658	15	73	33	9.0
LSS 2 & 8 *	791	14	86	45	9.0
LSS 3 & 7 *	130	3	19	7	1.5
LSS 4 *	508	5	313	11	8.7
LSS 6 *	232	0	49	7	6.1

* Half insertion

Table 11.3: Static heat in-leaks in distribution system (no contingency)

Temperature level		50-75 K [W]	4.6-20 K [W]	4.5 K LHe [W]	1.9 K LHe [W]	4 K VLP GHe [W]
Sector 1-2	QRL	10325	245	11	51	311
	Other *	500	190	-	-	45
Sector 2-3	QRL	9894	235	9	49	296
	Other *	95	67	-	-	29
Sector 3-4	QRL	9853	237	12	43	296
	Other *	156	93	-	-	34
Sector 4-5	QRL	10353	247	14	45	310
	Other *	746	198	-	-	34
Sector 5-6	QRL	10300	245	10	45	309
	Other *	586	183	-	-	34
Sector 6-7	QRL	9723	231	6	42	294
	Other *	156	93	-	-	34
Sector 7-8	QRL	9740	232	7	48	294
	Other *	156	93	-	-	34
Sector 8-1	QRL	10733	248	10	51	315
	Other *	586	183	-	-	34

* Interconnection boxes, local transfer lines and vertical transfer lines

Resistive heating

Resistive heating occurs in the non-superconducting sections of the magnet excitation circuits, essentially in splices of the superconducting cables and in current leads [33]. The heat load due to magnet splices has to be taken by the cold-mass helium bath. The residual resistances per splice assumed for heat load evaluation purposes depend on the type of circuit and on its location (Tab. 11.4). Resistive heating in current leads has to be taken by dedicated cooling circuits and helium baths in the electrical distribution feed boxes (DFBs). Tabs. 11.5 and 11.6 give the steady-state resistive heating in standard cells, arcs, dispersion suppressors (DS) and long straight sections (LSS) for nominal and ultimate operating conditions (see Sec. 11.6.1).

Table 11.4: Residual splice resistance assumed for heat load evaluation purposes [nΩ]

Magnet circuit	Nominal current [A]	Location		
		Inside magnet	Interconnection	
			Main	Others
MB	11850	0.5	0.6	-
MQ	11870	0.5	0.6	-
MCB	55	65		10
MS	550	1.4	7	10
MCBC	100	10	-	10
MCBR	100	10	-	10
MCBY	100	10	-	10
MCBXH	550	1	7	10
MCBXV	550	1	7	10
MQS	550	13	7	10
MQTL	550	1.4	7	10
MO	550	1.4	7	10
MCS	550	1.4	7	10
MCD	550	1.4	7	10
MCO	100	10	-	10

Table 11.5: Distributed steady-state resistive heating heat load in a standard cell [$W.m^{-1}$]

Temperature level	50-75 K	4.6-20 K	1.9 K LHe
Resistive heating nominal	0.02	0.003	0.10
Resistive heating ultimate	0.062	0.008	0.10

Table 11.6 : Steady-state resistive heating in cell, arc, DS and LSS

Temperature level		50-75 K [W]	4.6-20 K [W]	4.5 K LHe [W]	1.9 K LHe [W]	20-300 K [g/s]
Cell	nominal	2	0.3	-	11	-
	ultimate	7	1	-	11	-
Arc	nominal	43	7	-	248	-
	ultimate	153	19	-	251	-
DS 1, 2, 4, 5, 6 & 8 *	nominal	7	1	-	19	-
	ultimate	27	3	-	20	-
DS 3 & 7 *	nominal	7	1	-	18	-
	ultimate	27	3	-	19	-
LSS 1 & 5 *	nominal	1	0	24	3	8.0
	ultimate	3	0	24	3	8.0
LSS 2 & 8 *	nominal	1	0	26	3	8.3
	ultimate	3	0	25	4	8.3
LSS 3 & 7 *	nominal	1	0	2	1	2.4
	ultimate	3	0	2	1	2.4
LSS 4 *	nominal	1	0	16	2	8.5
	ultimate	3	0	16	2	8.5
LSS 6 *	nominal	-	-	11	1	6.3
	ultimate	-	-	11	1	6.3

* Half insertion

Beam-induced loads

Beam-induced heat loads are deposited in the cryo-magnets through several processes and by the circulating and colliding proton beams themselves. They depend strongly on the energy, the bunch intensity, number and length of the circulating bunches as well as on the luminosity in collision (Tab. 11.7). The various beam-induced loads are:

- synchrotron radiation from the bending magnet, mostly absorbed by the beam screens,
- resistive dissipation of beam image currents induced in the resistive walls and geometrical singularities of the beam channel,
- impingement of photo-electrons accelerated by the beam potential ("electron clouds"), mostly adsorbed by the beam screen,
- nuclear inelastic beam-gas scattering corresponding to a continuous distributed loss of particles from the circulating beam, mostly absorbed by the cold mass helium bath; this value is expected to decrease with running time due to improvement of the vacuum by beam cleaning,
- continuous random loss of particles escaping the collimation system, mostly absorbed by the cold mass helium bath over a length of a few tens of metres corresponding to the region of aperture restriction; in nominal conditions, the maximum random loss of particles per arc is 33 W with a maximum spread per cell of 3.4 W; in nominal conditions, the particle losses in the dispersion suppressor of the cleaning insertion (IR3 and IR7) is 33 W per half insertion.
- Losses of secondary particles, mostly absorbed at 1.9 K in the magnet cold-mass helium bath close to the high-luminosity experimental areas (inner triplet and dispersion suppressor cold masses); in nominal operation in a high-luminosity insertion secondaries are expected to deposit 182 W per half insertion in the inner triplet and 37 W per half-insertion in the dispersion suppressor;
- RF losses in superconducting acceleration cavities; in nominal conditions, RF losses are 200 W per half-insertion.

Tab. 11.8 gives the distributed steady-state beam-induced loads in and LHC cell for nominal and ultimate conditions. Tab. 11.9 gives the steady-state beam-induced loads in standard cells, arcs, dispersion suppressors (DS) and long straight sections (LSS).

Table 11.7: Scaling laws of beam-induced loads

Beam parameter	Energy E	Bunch current I_{bunch}	Bunch number n_{bunch}	Bunch length σ_z [r.m.s.]	Luminosity L
Resistive heating	E^2	-	-	-	-
Synchrotron radiation	E^4	I_{bunch}	n_{bunch}	-	-
Image current	-	I_{bunch}^2	n_{bunch}	$\sigma_z^{-3/2}$	-
Photo-electron cloud	-	I_{bunch}^3	n_{bunch}	-	-
Beam gas scattering	-	I_{bunch}	n_{bunch}	-	-
Random particle loss		I_{bunch}	n_{bunch}		
Secondaries	E	-	-	-	L
RF losses	-	I_{bunch}^2	n_{bunch}	-	-

Table 11.8: Distributed steady-state beam-induced loads in an LHC cell [mW m^{-1}]

Mode	Nominal		Ultimate	
Temperature level	4.6-20 K	1.9 K LHe	4.6-20 K	1.9 K LHe
Synchrotron radiation	330	1	500	1
Image current	360	1	820	2
Photo-electron cloud *	890	9	3040	30
Beam-gas scattering	0.4	48	0.4	48
Random particle loss	0-0.1	0-32	0-0.3	0-48
Total beam-induced *	1580	59-91	4360	82-130

* After beam cleaning

Table 11.9: Steady-state beam-induced loads in cell, arc, DS and LSS

Temperature level		4.6-20 K [W]	4.5 K LHe [W]	1.9 K LHe [W]
Cell	Nominal	169	-	6.3-9.7
	Ultimate	466	-	8.8-13.9
Arc	Nominal	3880	-	211
	ultimate	10740	-	284
DS 1 & 5 *	nominal	319	-	48
	ultimate	915	-	109
DS 2 & 8 *	nominal	319	-	12
	ultimate	914	-	18
DS 3 & 7 *	nominal	354	-	44
	ultimate	1037	-	70
DS 4 & 6 *	nominal	319	-	11
	ultimate	914	-	16
LSS 1 & 5 *	nominal	45	10	193
	ultimate	118	22	440
LSS 2 & 8 *	nominal	37	6	41
	ultimate	100	12	95
LSS 3 & 7 *	nominal	21	1	0
	ultimate	61	1	1
LSS 4 *	nominal	31	214	2
	ultimate	87	529	2
LSS 6 *	nominal	3	7	-
	ultimate	4	14	-

* Half insertion

11.4.2 Transient Modes

Ramping the magnetic fields up and down will generate additional transient heat loads in the superfluid helium due to the eddy currents developed in the superconducting cables and in the mechanical structure of the magnets. Raising the current to its nominal value in 1200 s is expected to dissipate 480 J of energy per metre length of main dipole. This represents a power of approximately 0.4 W per metre. In the case of a resistive transition or in an emergency, it must be possible to ramp the full current down to zero in 80 s. This will result in an energy dissipation of 3000 J per metre of magnet. This represents a power of approximately 38 W per metre.

The only practical way to absorb these transient heat loads and keep the temperature below 1.9 K during ramping-up and below the lambda line during fast ramp-down is to make use of the heat capacity of the liquid helium contained in the magnet cold-masses. About 15 l of liquid helium per metre length is sufficient to cope with the loads to be buffered.

11.5 COOLING SCHEME

11.5.1 Arc and Dispersion Suppressor Cooling Loops

The corresponding flow-scheme of a lattice cell appears in Fig. 11.5. The first level of thermal shielding and heat interception in the magnet cryostats and the distribution line is provided by forced circulation of gaseous helium under pressure at a temperature between 50 K and 75 K, through headers E and F respectively. The cryo-magnets operate in a static bath of pressurised helium II (grey area), cooled by heat exchange with flowing saturated helium II. Low-pressure vapour resulting from the vaporisation of the saturated helium II is returned to the refrigerator by header B. Supercritical helium is distributed by header C and is used to; a) fill the cryo-magnet baths, b) produce - after subcooling and Joule-Thomson expansion -

the saturated helium II flowing in the full cell length heat exchanger tube and c) feed line C' that cools the cold heat intercepts in the support posts at about 5 K, in series with the beam screens that operate between about 5 K and 20 K. The resulting gaseous helium is returned to the refrigerator by header D.

The large, but finite bulk thermal conductivity of static pressurised superfluid helium has been successfully applied for cooling devices below 2 K and transporting their heat loads over distances of up to a few tens of metres. Cooling the kilometre-long strings of magnets in the LHC sectors within a narrow temperature range, say 0.1 K, is however beyond the capability of helium-II thermal conduction alone [34]. In order to maintain the furthest magnet of each sector below 1.9 K, each 106.9 m-long LHC cell is composed of a single bath of static pressurised superfluid helium, cooled from a quasi-isothermal heat sink in the form of a bayonet heat exchanger running through the magnet string [35] and in which the latent heat of a stratified two-phase flow of saturated helium II absorbs the applied heat load, about 0.4 Wm^{-1} in the LHC arc.

The performance of such a scheme critically depends on the thermo-hydraulic behaviour of two-phase helium II flowing in quasi-horizontal tubes: this has been the subject of theoretical modelling and experimental studies at CERN [36] and CEA Grenoble (France) [37, 38, 39]. These studies have demonstrated that over a large range of vapour quality, most of the tube cross-section is occupied by the vapour flow, which then controls the overall pressure drop. For vapour velocities of up to a few m s^{-1}, the drag between the two phases remains small, so that the liquid flows separated from the vapour, almost as if in single phase and open channel. In this condition, the heat transfer is mainly controlled by the wetted area inside the tube, which can be adequately predicted by simple models for engineering purposes. Other important factors controlling the heat transfer across the tube wall are the conductivity of the tube material and the Kapitza thermal resistance at the solid-liquid interfaces [40]. By using a 53.4 mm inner diameter tube of OFHC copper with a wall thickness of 2.3 mm, the total transverse impedance when fully wetted can be kept down to about 0.3 mK m^2 W^{-1}, and the practical heat transfer capability of the partially wetted bayonet heat exchanger is thus typically a few mK m W^{-1}. The final validation of this cooling scheme was performed on a full scale magnet string which has accumulated about 8'000 hours operation at 1.9 K, successfully undergoing all possible nominal and off-design operating conditions [41]. This full scale working model of a LHC cell enabled the dynamic control aspects to be addressed. These are particularly demanding on this system characterised by strong non-linearities - including initial inverse response - and long time delays induced by the low velocity of the liquid flow. To cope with this, advanced automation techniques [42] such as linear model-based predictive control [43] is considered as an alternative to standard PID controllers.

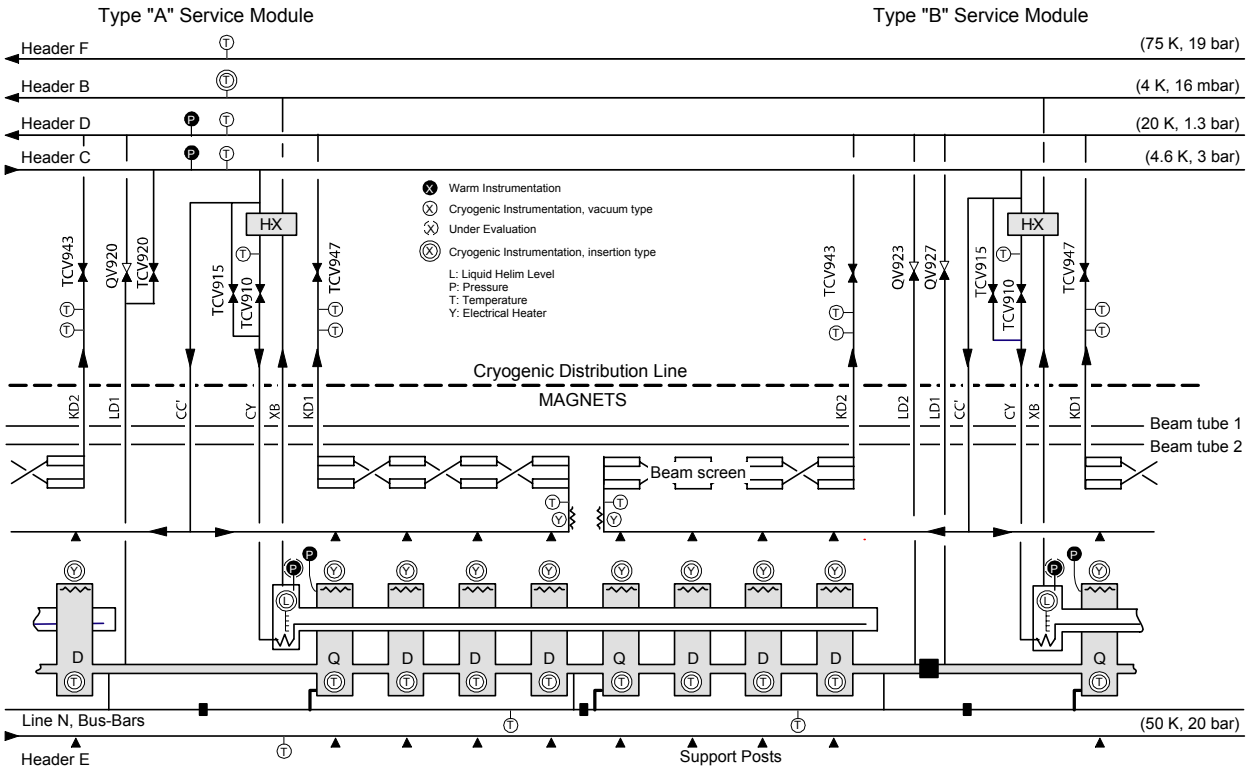

Figure 11.5: Cryogenic flow-scheme and instrumentation of a LHC lattice cell

Cryogenic sub-sectorisation

Within a sector the tunnel slope results in elevation differences up to 50 m, which would develop a large hydrostatic head of up to 70 kPa (700 mbar) in the corresponding string of cold masses, if the cold masses were to remain hydraulically connected. Depending on the pressure normalisation point, this hydrostatic head could increase the helium leak rate across the seat of cold safety relief valves and consequently the heat load on the cold-masses. It could also create sub-atmospheric pressure in some part of the magnet string with risk of the pollution by air in-leaks. To limit the enhancement of valve leak rate and to avoid parts of the cold mass going sub-atmospheric, the cold mass volume within a sector has been sub-sectorised by adding hydraulic restrictions every two or three cells (Fig. 11.6). These hydraulic restrictions also restrict the propagation of resistive transition, caused by warm helium flow from magnet to magnet, to the magnets of one hydraulic sub-sector.

The cryogenic vacuum is also sub-sectorised in order to limit the extent of a degraded vacuum zone created by a possible helium leak of the internal circuit. On the cryo-magnet side, vacuum barriers are integrated in the Short Straight Section cryostats every two cells. On the cryogenic distribution line side, vacuum barriers are integrated every four cells. The jumper connection between QRL and magnet cryostats always contains a vacuum barrier.

Together, these two sub-sectoring schemes for cold mass and insulation vacuum allow a limited length of cryo-magnets (up to 600 m) to be warmed up and short interventions on the cold-mass components (splices, diodes, 60 A current leads…) to be made. In this case, the warm-up and re-cool-down time is reduced by a factor three with respect to the normal full sector warm-up and cool-down times. However, for removing cryo-magnets, which require the opening of cold bores or bayonet heat exchangers or main headers, the complete sector has to be warmed up and re-cooled.

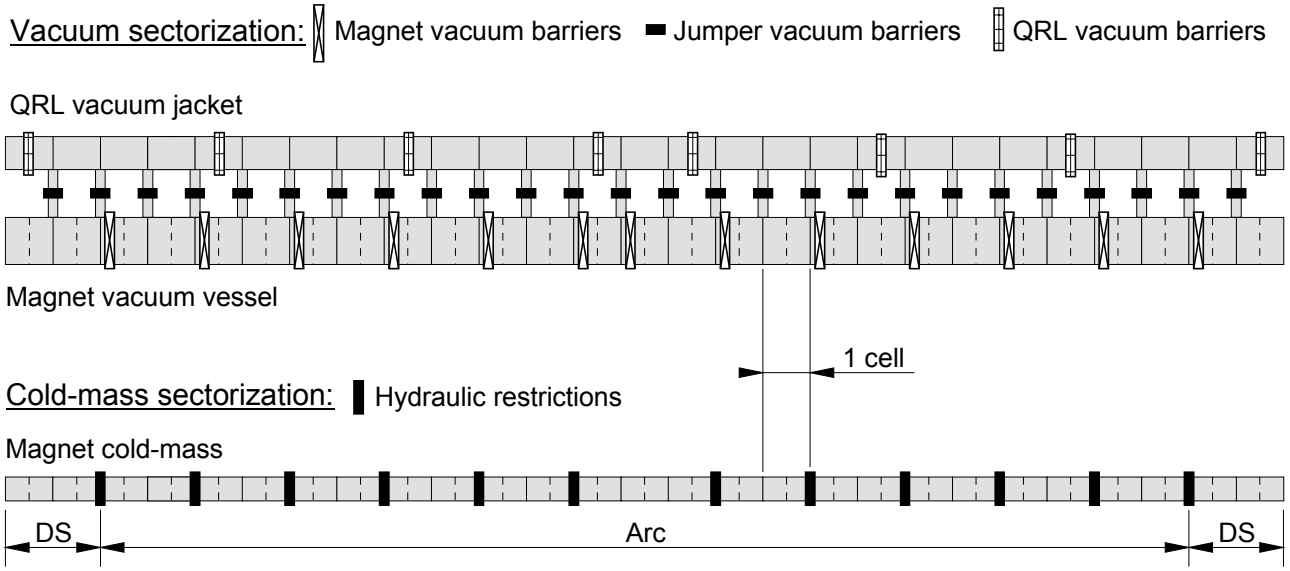

Figure 11.6: Cold-mass and cryogenic vacuum sub-sectorisation

11.5.2 Matching Section Cooling Loops

The special magnets of the matching section (see Chap. 8), which do not require cooling at 1.9 K for field strength and heat extraction, operate in baths of saturated helium I at 4.5 K. The cryostats are referred to as standalone or semi-standalone, because they generally never consist of more than one quadrupole or dipole magnet cryostat plus correctors (standalone) or a quadrupole and dipole magnet cryostat in series plus correctors (semi-standalone). The quadrupole and dipole magnets themselves are very diverse, corresponding to their specific functions in the LHC machine optics. Although the detailed cryogenic schemes have to be in accord with this diversity they all share the characteristics depicted in Fig. 11.7. There is an actively cooled heat intercept at about 70 K. The cold mass is filled and the liquid level actively maintained by helium supply from QRL header C. The vapour outlet is into QRL header D, whose pressure of about 0.13 MPa

(1.3 bar) directly determines the corresponding magnet's saturated liquid bath temperature at about 4.5 K. The vapour outlet is always in open connection to QRL Header D, thereby eliminating the need for a safety valve. If a magnet experiences a resistive transition, the helium is expelled directly into header D. The open connection does, however, require collective warm-up of all 4.5 K operated magnets of the corresponding sector when header D becomes exposed to atmosphere, e.g. due to repair. In nominal operation the beams screens are actively maintained in a temperature range of 5 K to 20 K by a flow of supercritical helium at about 0.3 MPa (3 bar) taken from header C and exiting into header D. To prevent unbalanced cooling of the apertures, the beam screen cooling circuits are always in series.

Instrumentation for temperature and/or pressure of the helium streams is placed in the QRL service module whenever possible. The liquid level gauge and temperature sensor in the magnet cryostat are extractable which eliminates the need for installing redundant ones. The temperature sensor is required only for monitoring the cool-down speed. Furthermore, there is a warm-up heater inside the cold mass and a heater plus its corresponding temperature sensor on the beam screen cooling circuit inlet. In nominal operation the beam screen heater serves to prevent density wave oscillations in the beam screen flow.

The standalone and semi-standalone magnets receive their powering through a dedicated interface which in the majority of cases connects to a local current feed box (DFBM) or else to a superconducting link (DSL). The electrical connection is via a special feed-through that as well as providing electrical insulation also hydraulically separates the magnet's helium bath from the helium in the DFBM and/or DSL. All necessary cryogens for the DFBM and part of the cryogens for the DSL are routed through the magnet cryostat to the QRL.

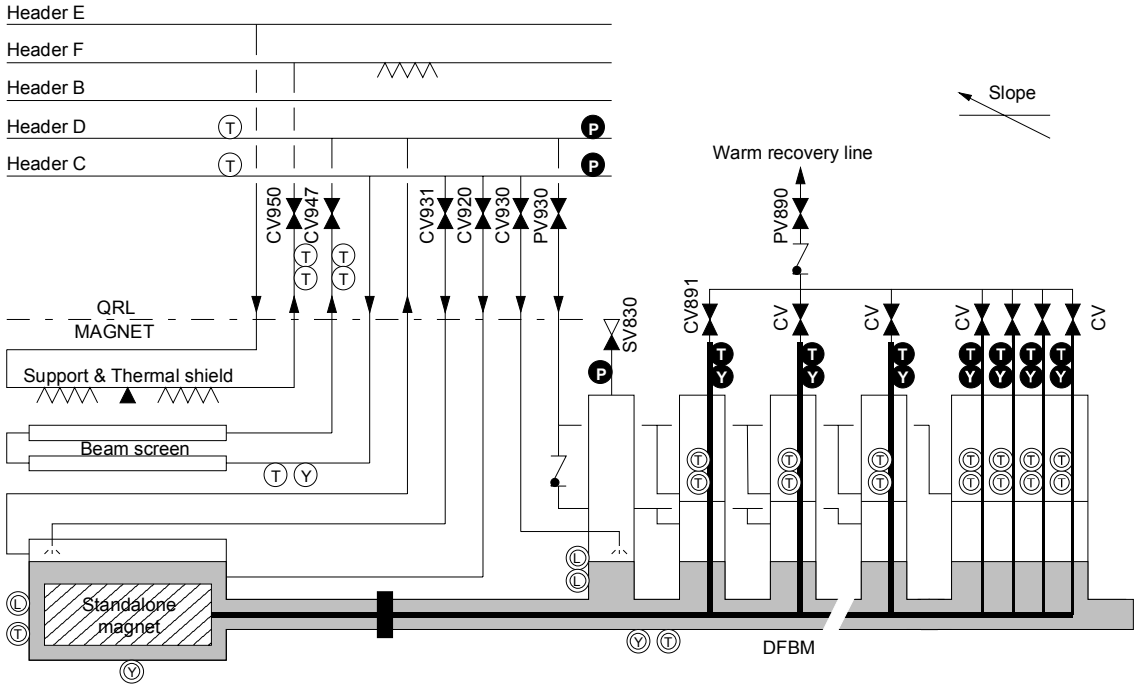

Figure 11.7: Cryogenic flow-scheme and instrumentation of a 4.5 K standalone magnet

11.5.3 Inner Triplet Cooling Loops

The inner-triplet quadrupoles in the insertion regions are subject to dynamic heating from secondaries of up to 10 W m^{-1} at each of the high luminosity insertions 1 and 5 and up to about 2 W m^{-1} at the low luminosity insertions 2 and 8 from the particle interactions. Although this represents a much higher heat load than the magnets in the arc and DS receive, they can be cooled by a scheme similar to the standard cell. A large-diameter, corrugated copper heat exchanger tube inside a stainless steel pipe will be placed outside of and parallel to the cold mass in the cryostat [44]. A full-scale experimental set-up modelling this cooling loop, designed and built by FNAL Batavia (U.S.A.), has validated the cooling method [45]. The present implementation is more than sufficient for nominal LHC luminosity. For ultimate luminosity the system needs to be upgraded. The bottlenecks are mostly in the longitudinal conduction path from the magnet coil to the overcrowded interconnect and then to the parallel heat exchanger.

The superconducting single aperture beam separation dipoles D1 installed in the low luminosity insertions will operate at 1.9 K and will be cooled almost exactly as the arc and DS magnets. The only notable difference is that because of space limitations, two parallel bayonet heat exchangers of straight copper pipe but of smaller diameter will be used instead of a single one. The choice of operating temperature is mainly determined by maximum aperture requirements. Using a RHIC type dipole (originally designed to operate in forced flow supercritical helium of about 5 K) at 1.9 K, it was possible to safely increase the beam pipe diameter to the mechanical maximum.

Fig. 11.8 shows the cryogenic flow-scheme and instrumentation for a high luminosity insertion inner triplet.

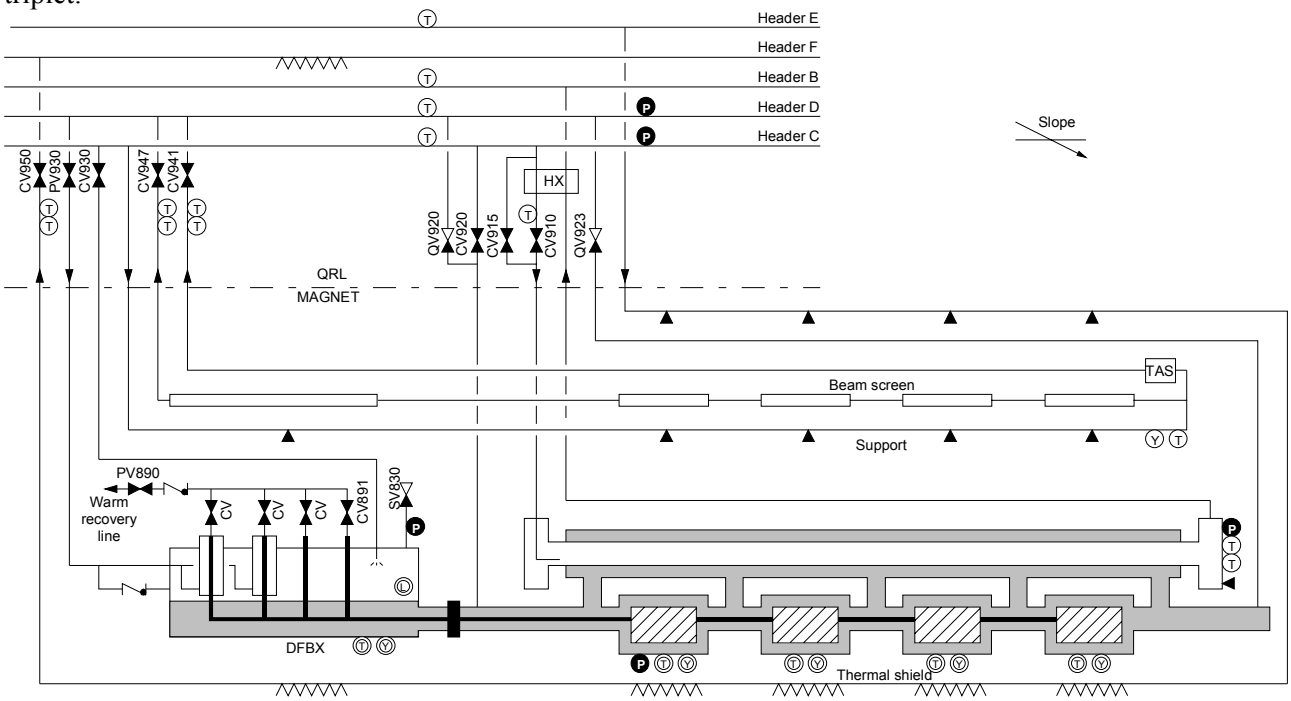

Figure 11.8: Cryogenic flow-scheme and instrumentation of an inner triplet cell

11.5.4 Electrical Distribution Feed Box and RF Cavity Cooling Loops

The electrical distribution feed boxes (DFBAs, DFBMs, DFBLs and DFBXs) (see Chap. 9) and the RF cavities (see Chap. 6) are low design pressure equipment (0.35 MPa for the DFBs and 0.25 MPa for the RF cavities) connected to high design pressure (2 MPa) equipment and cryogen supplies. This peculiarity has specific consequences for their cryogenic implementation. A typical DFB and the RF flow scheme are given in Figs. 11.9 and 11.10.

With the exception of the DFBMs all DFBs have an actively cooled 70 K thermal screen. The lower part of the DFB current leads [46] and busbar bundles are in saturated liquid helium baths which have a common liquid level regulation. The upper, resistive part of the HTS leads is cooled by gaseous helium between 20 K and ambient temperature. Liquid for the saturated helium baths is taken from QRL header C, and vapour is returned to a collector which connects QRL header D to the 20 K gaseous helium inlet of the HTS leads. A non return valve is placed between this collector and the saturated liquid bath to prevent high temperature gas inadvertently entering the liquid bath space. The 20 K helium supply for the resistive part of the HTS leads consists of the bath evaporation complemented with helium from QRL header D. The helium is returned at ambient temperature to the warm recovery line. These flows are controlled at ambient temperature by lead specific valves. To protect the DFBs from overpressure from header D a pressure controlled shut-off valve is placed in the connection to QRL header D. Protection from overpressure in the warm recovery line is provided by a non-return valve. Protection from pressure differences over the control valve in excess of 50 kPa (500 mbar) is provided by a pressure control valve in the warm recovery line connection. Discharge of any helium contained in enclosed DFB spaces will be into the LHC tunnel. In the event of header D pressure shut-off valve failing, the flow rate from header D into the tunnel and the DFB pressure build up are restricted by design of the connecting piping.

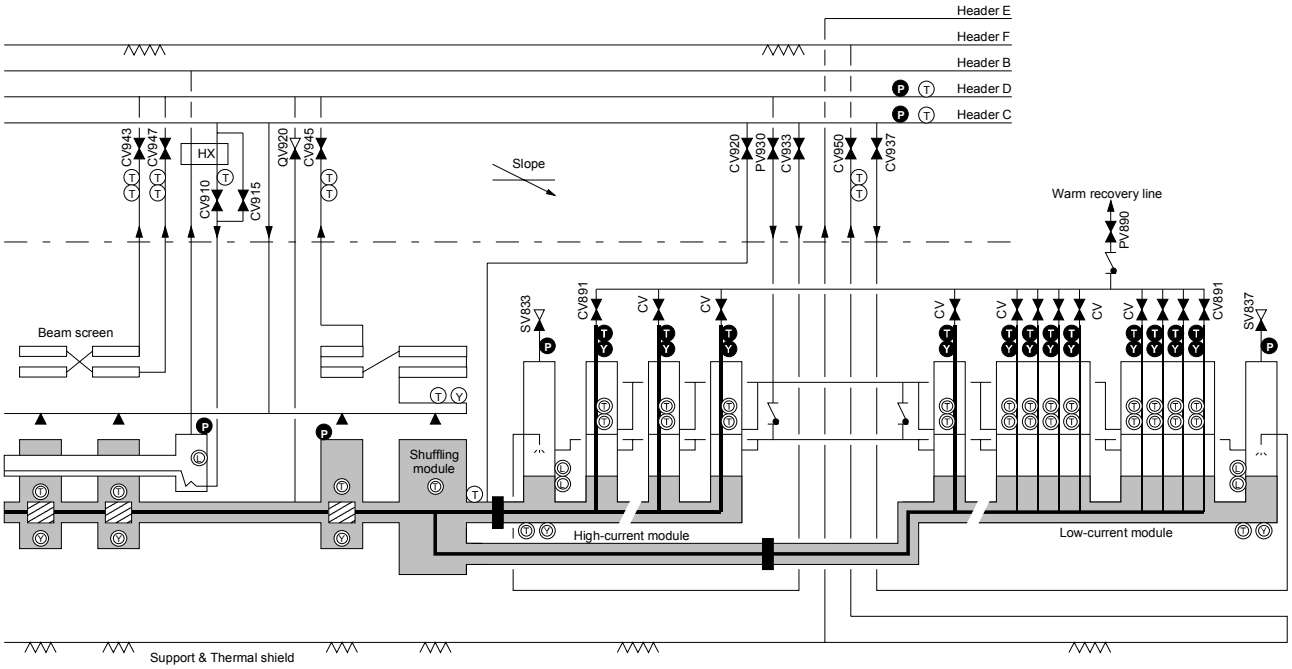

Figure 11.9: Cryogenic flow-scheme and instrumentation of a DFBA type electrical distribution box

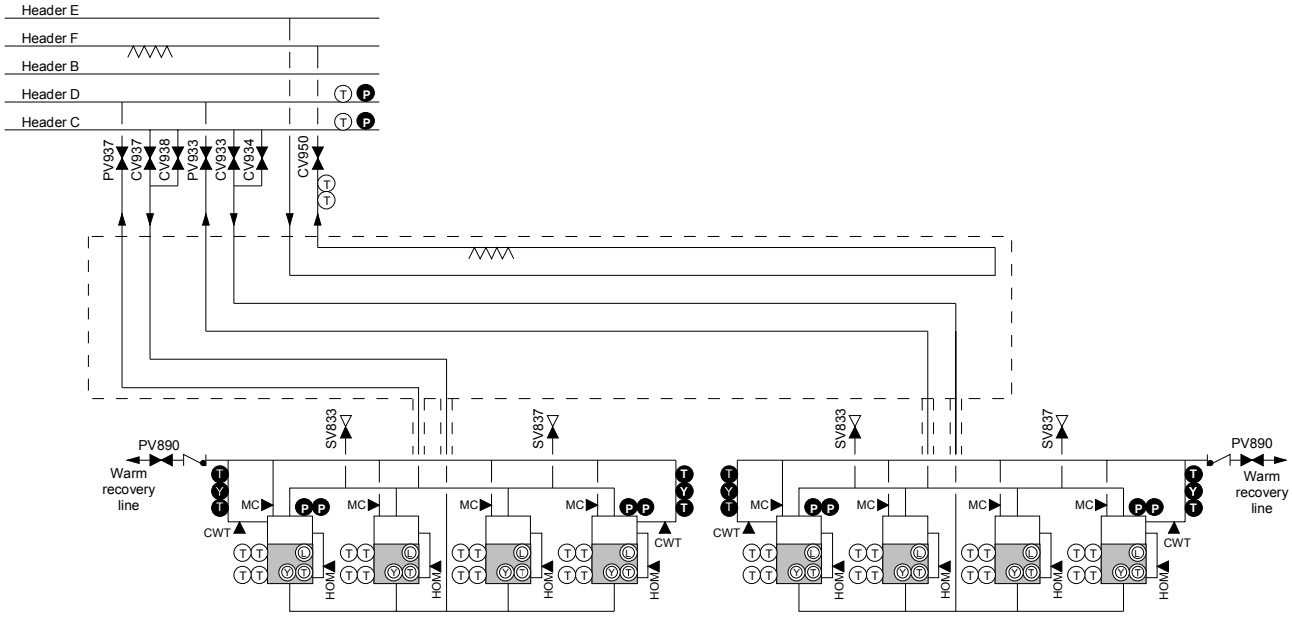

Figure 11.10: Cryogenic flow-scheme and instrumentation of an RF cavity assembly

11.6 OPERATING MODES

11.6.1 Steady-state Operation

Four steady-state operating modes and their corresponding requirements for the cryogenic operation of the machine are considered:

- 'nominal operation' at 7 TeV beam energy, 2×0.582 A beam current and 10^{34} cm^{-2} s^{-1} luminosity.

- 'ultimate operation' at 7 TeV beam energy, 2 × 0.86 A beam current and $2.5 \cdot 10^{34}$ cm^{-2} s^{-1} luminosity, assuming a two-fold reduction of residual pressure in the beam channel over long term operation.
- 'low beam intensity operation', characterised by negligible beam-induced heat loads in the magnets but still with full beam energy and thus full excitation current in the magnets.
- 'injection standby' characterised by negligible resistive dissipation and beam-induced heat loads in the magnets.

Cryogenic cooling powers required for each operation mode are given in Tab. 11.10. For efficient operation, large turndown capability is required for the refrigeration plants.

From Tab. 11.10, two sector types are identified. The sectors 1-2, 4-5, 5-6 and 8-1, which include high-luminosity insertions are identified as 'high-load' sectors. The other sectors, less demanding in cryogenic capacity are identified as 'low-load' sectors.

The temperature profiles of the LHC sectors can be calculated with confidence for the various operation modes based on the measured performance of the cooling loop (Fig. 11.11). This shows that the demanding requirement of 0.1 K in nominal operation between the furthest cryo-magnet and the sector refrigerator can be met.

Table 11.10: Cryogenic capacity requirements for each steady-state operating mode (no contingency)

Temperature level		50-75 K [kW]	4.6-20 K [W]	4.5 K LHe [W]	1.9 K LHe [W]	4 K VLP GHe [W]	20-300 K [g/s]
Injection Standby	Sector 1-2	24.9	843	170	667	356	18
	Sector 2-3	23.6	698	114	639	325	11
	Sector 3-4	23.3	717	344	599	330	10
	Sector 4-5	24.9	844	400	627	344	18
	Sector 5-6	24.4	822	132	623	343	15
	Sector 6-7	22.9	706	74	594	328	8
	Sector 7-8	23.5	721	112	638	328	11
	Sector 8-1	25.4	839	169	667	349	18
Low beam-intensity	Sector 1-2	25.0	852	220	959	356	34
	Sector 2-3	23.6	707	142	928	325	21
	Sector 3-4	23.4	726	362	887	330	21
	Sector 4-5	25.0	853	440	918	344	34
	Sector 5-6	24.5	831	167	913	343	29
	Sector 6-7	23.0	715	87	881	328	16
	Sector 7-8	23.5	730	140	927	328	21
	Sector 8-1	25.5	848	197	956	349	29
Nominal	Sector 1-2	25.0	5450	236	1460	356	34
	Sector 2-3	23.6	5320	149	1240	325	21
	Sector 3-4	23.4	5330	577	1160	330	21
	Sector 4-5	25.0	5450	664	1380	344	34
	Sector 5-6	24.5	5400	184	1380	343	29
	Sector 6-7	23.0	5290	95	1150	328	16
	Sector 7-8	23.5	5340	147	1240	328	21
	Sector 8-1	25.5	5450	213	1460	349	29
Ultimate	Sector 1-2	25.0	13600	254	1910	356	34
	Sector 2-3	23.6	13600	155	1400	325	21
	Sector 3-4	23.4	13600	892	1260	330	21
	Sector 4-5	25.0	13600	991	1770	344	34
	Sector 5-6	24.5	13500	203	1760	343	29
	Sector 6-7	23.0	13500	102	1250	328	16
	Sector 7-8	23.5	13600	153	1400	328	21
	Sector 8-1	25.5	13600	231	1900	349	29

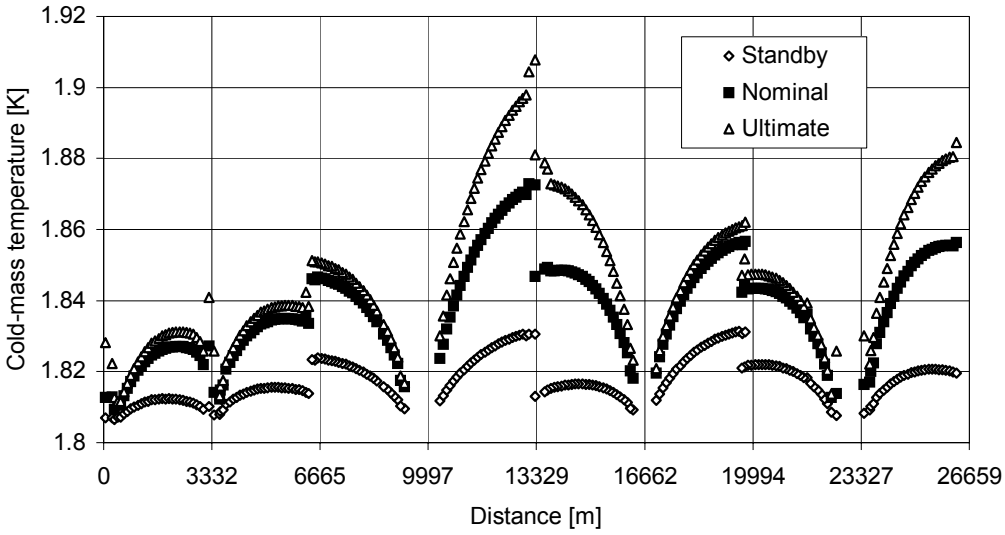

Figure 11.11: Calculated temperature profiles of LHC magnets

11.6.2 Transient Modes

Four transient modes are considered: cool-down from 300 K to 4.5 K, magnet filling and cool-down from 4.5 K to 1.9 K, resistive transition and warm-up from 4.5 K to 300 K.

Cool-down from 300 K to 4.5 K

Cooling of the magnets from ambient temperature is carried out by forced circulation of gaseous helium. To be able to cool-down the cold mass of a LHC sector in a maximum time of 15 days, liquid nitrogen pre-coolers with a maximum capacity of 600 kW are installed in each refrigeration plant. They are either integrated into the new 4.5 K refrigerator cold-boxes or added as auxiliary equipment to the upper cold-boxes (in the 4.5 K refrigerators recovered from LEP). These pre-coolers progressively decrease the temperature of a 770 g s^{-1} gaseous helium flow, with a maximum temperature difference between the supply and return streams of 150 K. The pre-coolers produce effective refrigeration capacity down to 80 K. Below this temperature, the cool-down capacity is provided by the turbo-expanders of the refrigerators. To avoid a longitudinal thermal gradient in the cryo-magnet structure higher than 75 K, a progressive initial ramp-down on the inlet temperature is applied. Normal cool-down is performed using one refrigeration plant (Fig. 11.12). Fast cool-down, reducing by two the normal cool-down time, can also be performed by using two refrigeration plants coupled to one sector, except in sector 2-3 [47, 48].

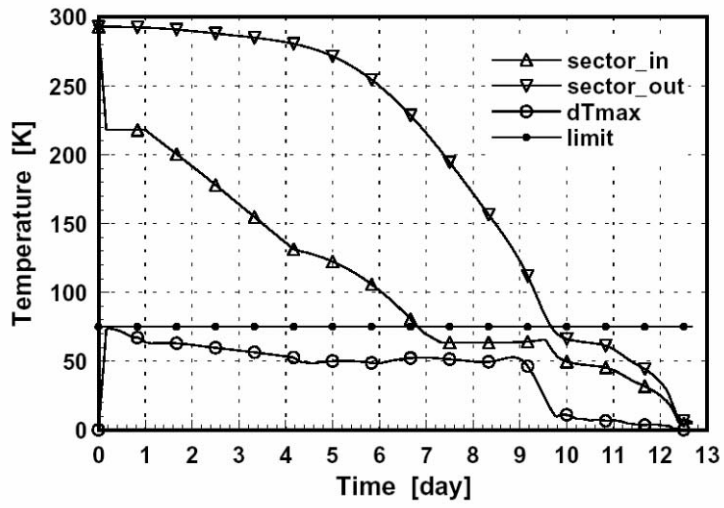

Figure 11.12: Normal cool-down from 300 K to 4.5 K of LHC sectors

Magnet filling and cool-down from 4.5 K to 1.9 K

The filling of the magnets is performed in two steps. The first step uses the liquefaction capacity of the 4.5 K refrigerators to partially fill the cold mass volume with saturated helium at 4.5 K up to the level determined by the position of the highest interconnecting pipe. The filling of the remaining dead volume is performed using the 1.8 K refrigeration unit which condenses the remaining gaseous helium at constant pressure of about 0.1 MPa (1 bar).

Once the magnets are filled, the cool-down to 1.9 K is performed using the 1.8 K refrigeration units. Depending of the number of refrigeration plants coupled to one sector, normal or fast operation can be performed (Fig. 11.13) as is the case for the cool-down from ambient,.

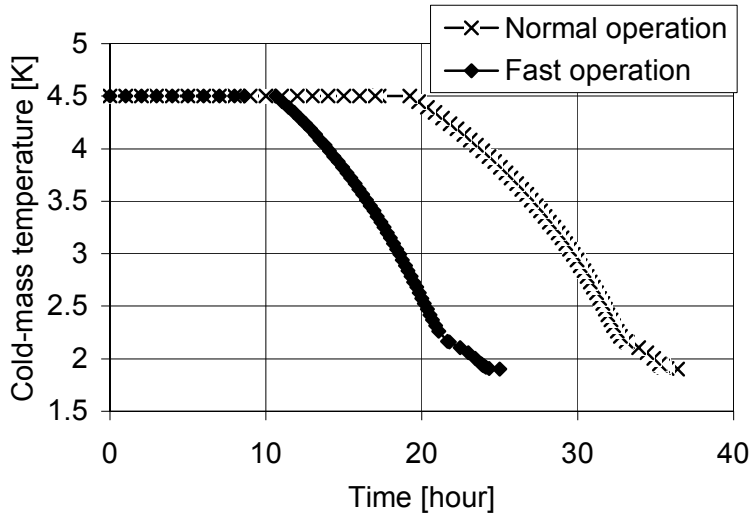

Figure 11.13: Magnet filling and cool-down down from 4.5 K to 1.9 K

Resistive transition

In the first few tenths of a second following the transition of a dipole magnet, the 500 kJ m^{-1} stored magnetic energy is dissipated in the resistive windings, and part of it eventually released to the static helium in the cold mass on a much longer time scale. To contain the resulting pressure rise within the 2 MPa (20 bar) design pressure of the helium enclosure, helium has to be discharged at high flow-rate into header D, normally kept cold by the 20 K bleed from the beam-screen cooling circuits. The large acceptance of this header enables it to perform as a temporary buffer storage, thus avoiding the need for further helium discharge in case of resistive transitions affecting limited stretches of magnets (one to several lattice cells) [49,50]. For generalised resistive transitions, cold gaseous helium is discharged and recovered, though at much lower flow-rates, from header D into the 2 MPa (20 bar) gas storage vessels at ambient temperature which are located in the service areas at the surface areas around the LHC circumference [51].

The discharge of helium from the magnet cold mass is made possible, every 106.9 m, by some 400 cold safety relief valves, normally closed, with their inlet under pressurised helium II. Such components, which are not available off-the-shelf, had to be developed by industry following CERN specifications [52] and their performance assessed on a specially designed test facility [53].

The thermo-hydraulic consequences of resistive transitions in the cryo-magnets may constitute a significant, but not exclusive source of risk to personnel or equipment. Its mechanism however is well understood and the cryogenic infrastructure is designed to cope with it. A systematic risk assessment in the cryogenic system, based on an analysis of the occurrence of accidental events and the gravity of their consequences, has been recently conducted [54, 55, 56, 57, 58]. It confirmed the strong contribution to the intrinsic safety of the specific design features of the system, such as the large acceptance of the cold recovery header D, the absence of liquid nitrogen underground and of helium pumps in the cooling loops.

The re-cool-down time after a resistive transition of limited stretches of magnet is between 2 and 6 hours (Fig. 11.14).

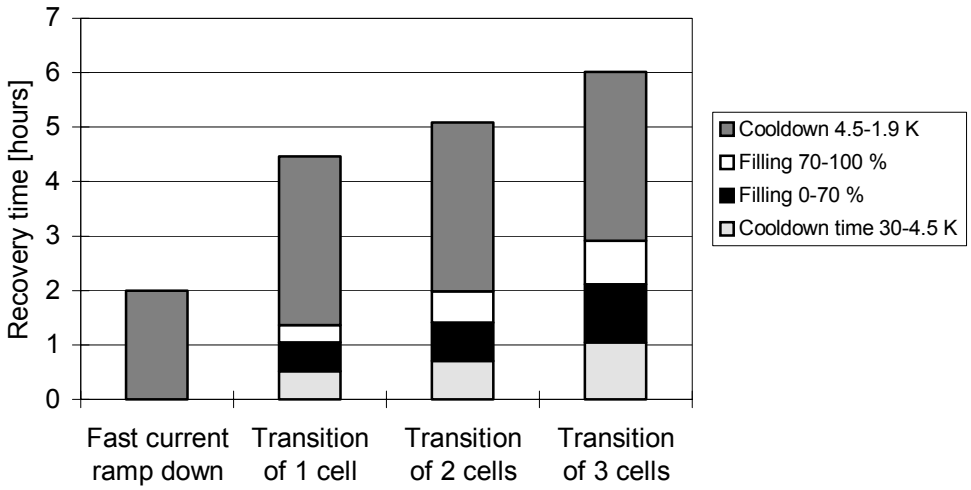

Figure 11.14: Magnet re-cool-down after a limited resistive transition

Warm-up from 4.5 K to 300 K

Warming of the magnets to ambient temperature is carried out by forced circulation of gaseous helium. To be able to warm-up the huge cold mass of a sector in a maximum time of 15 days, electrical heaters with a maximum capacity of 600 kW are integrated into the interconnection boxes of the refrigeration plants. These heaters progressively increase the temperature of a 770 g s^{-1} gaseous helium flow with a maximum temperature difference between the supply and return streams of 150 K. To avoid longitudinal thermal gradients in the cryo-magnet structure higher than 75 K, a progressive initial ramp-up on the inlet temperature is applied. Normal warm-up uses one refrigeration plant (Fig. 11.15). With the exception of sector 2-3, fast warm-up in half the normal warm-up time can also be performed by using two refrigeration plants coupled to one sector.

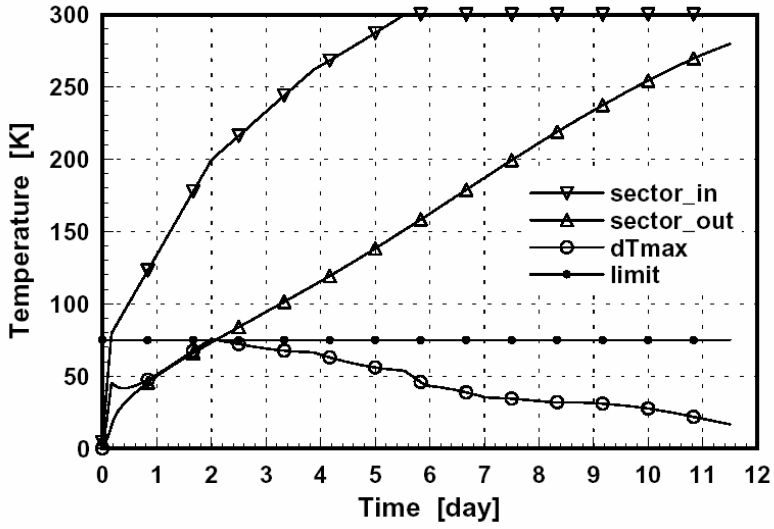

Figure 11.15: Normal warm-up of LHC sectors

11.7 CRYOGENIC DISTRIBUTION

The central nodes of the cryogenic distribution system are situated in the underground caverns. These are the cryogenic interconnection boxes (QUIs) which provide the connection between the different cryogenic sub-systems at each of the five feed-points: surface 4.5 K cold boxes (QSRB) underground 4.5 K lower cold-boxes (QURA), 1.8 K refrigeration unit boxes (QURC), and cryogenic distribution line (QRL).

The upper cold boxes of the new 4.5 K refrigerators are linked to the interconnection boxes via four vertical helium transfer lines (QPLB) passing through the main LHC shafts. These QUIs are located between 80 m and 145 m underground depending on the access point. The lower cold boxes of the refrigerators recovered from LEP and those of the 1.8 K refrigeration units are connected to the interconnection boxes via 12 underground helium transfer lines (QUL). A cryogenic distribution line (QRL) feeds helium at different temperatures and pressures the elementary cooling loops of the cryomagnets and other devices for each of the eight sectors, starting from the QUI and running all along the tunnel. The QUL, QPLB and QRL consist of three, four or five internal process pipes, hereafter referred as headers. The headers are housed in a common vacuum jacket and a common actively-cooled thermal shield. To reduce the heat in-leaks from ambient, the thermal shield and the cold supply headers are wrapped with blankets of reflective multilayer super-insulation and the supporting spacers made of fibre-glass composite materials.

The QPLB (vacuum jacket DN600) [59] are between 90 m and 190 m long and each of them has four headers (DN80 to DN150). The main part of the QPLB is a vertical straight segment between 75 and 125 m long. Because of limited accessibility and for maximum reliability, no internal or external bellows or bends have been accepted in this part. Hence, all thermal contraction is taken in a thermal compensator specified to be at ground level. For the longest line, the thermal compensator must take more than 35 cm displacement. Each header will be equipped with two horizontal angular bellows and one vertical angular bellows. The vertical part of the line has a sliding point directly below the compensator and a fixed point at the bottom 125 m below.

The QUL vacuum jacket which is connected to the 1.8 K refrigerator units (DN500) houses three headers (DN40 to DN250). The QUL vacuum jacket linked to the refrigerators recovered from LEP (DN600) houses four headers of the same dimensions as for the QPLB. Depending on the relative position of the components to connect, the length of these lines can vary from 5 m to 30 m. Dedicated shuffling boxes are needed at the interface to the cold boxes as the lines coming out of them are not grouped on a common standard interface, but in six different outlets. Each of the outlets consists of a single cryogenic line housing one or two process pipes. These shuffling boxes comprise separate single cryogenic lines as well as vacuum barrier(s), elbows and DN700 line portions necessary to bring together the different outlets in one compound transfer line which is then connected to the QUI. At the interfaces to the QUI and QURC, smaller shuffling boxes may be needed allowing for a re-arrangement of the position of the headers within the vacuum enclosure according to the orientation of the interfaces defined for CERN equipment.

The QRL sector [60] is a continuous cryostat of about 3.2 km length without any header sub-sectorisation, but divided into nine vacuum sub-sectors. A QRL sector starts at the QUI and ends at the return modules on the opposite side where the different headers are interconnected to form continuous cooling loops. The QRL, following the LHC lattice, is a repetitive pattern of pipe modules (about 100 m) and service modules (about 6.6 m), which link the QRL to the magnet cryostats once at every full cell (see Fig. 11.1). The arc is made of 22 identical cells, each of 106.9 m length. The DS is made up of four QRL cells of with lengths varying from 79 m to 93 m. The LHC lattice in each LSS is very different, with QRL cell lengths from about 10 m to 115 m. Five headers (inner diameters 80 mm to 269 mm) are housed in the QRL (outer diameter 650 mm) running along the LSS. Inside the arc and DS the supply header E is housed inside the LHC magnet cryostats while the return header F is always inside the QRL. A service module houses the subcooling heat exchanger, all cryogenic control valves for the local cooling loops, one or two cold safety relief valves as well as the necessary monitoring instrumentation. The so-called jumper connection, part of the service module, houses up to nine tappings (diameter 10 mm to 80 mm) to and from the magnet cryostats and a transverse vacuum barrier separating the QRL from the magnet string vacuum systems. All interconnecting pipes as well as the vacuum jacket are equipped with flexible elements to minimise forces applied to the precisely aligned cryo-magnets by the QRL and to allow re-alignment of the magnet strings without displacement of the QRL. In order to realign machine elements without moving the QRL, the jumper connections must be able to compensate for movements of the beam tubes relative to the QRL up to ± 25 mm in the horizontal plane and ± 50 mm in the vertical direction.

Due to different cryogenic users and flow-scheme peculiarities, 44 different types of service modules are required. Most of the variants are inside the LSS.

A QRL sector comprises about 240 straight pipe elements, 40 fixed point/vacuum barrier elements, 37 service modules, 1 test module (used for reception test only), one return module, two to three doglegs, two elbows and 320 interconnections (including about 400 compensation units). A standard pipe module consists of eight straight pipe elements (about 11.3 m), one fixed point element (about 6.6 m) located in the

centre and compensation units. Different QRL cell lengths and routing singularities (e.g. departure from the LHC tunnel towards the QUI located inside a cavern) will be accommodated by special pipe elements of non-standard length or an elbow. To match the tight thermal budget the design had to be highly optimised. The QRL is a largely modular ensemble of pipe and service modules and therefore it allows a high degree of standardisation and consequently series production of various elements.

11.8 REFRIGERATION PLANTS

11.8.1 Installed Refrigeration Capacity

The refrigeration capacity of the sectors [61], listed in Tab. 11.11, includes contingency for excess capacity and uncertainty in heat load budgets for the nominal operation mode and allows the ultimate operation mode according to the heat load level assumed in 1997 without contingency. These values were used for specifying the new 4.5 K refrigerators and the 1.8 K refrigeration units. Since the ordering of the refrigerators, the electron cloud heat load prediction has increased by more than a factor 4. Consequently, the installed capacity for the temperature level 4.6-20 K does not cope with the presently estimated demand in ultimate conditions (about 13.5 kW per sector), but still fulfils the nominal demand (about 5.3 kW per sector).

Table 11.11: Installed refrigeration capacity in the LHC sectors

Temperature level		High-load sector	Low-load sector
50-75 K	[W]	33000	31000
4.6-20 K	[W]	7700	7600
4.5 K	[W]	300	150
1.9 K LHe	[W]	2400	2100
4 K VLP	[W]	430	380
20-280 K	[$g.s^{-1}$]	41	27

11.8.2 4.5 K Refrigerators

The refrigeration of the LHC sectors requires mixed-duty operation of the cryogenic helium refrigerators, in order to fulfil a variety of isothermal and non-isothermal cooling duties. This amounts to a total equivalent entropic capacity of 144 kW at 4.5 K, thus making the LHC the world's most powerful helium refrigeration system.

Previous experience at CERN with large cryogenic helium plants delivered by European industry in the framework of turn-key contracts, has demonstrated their dependable performance, good efficiency and high operational reliability [62]. Consequently in 1997 CERN issued a functional and interface specification for the procurement of four new such refrigerators to equip the "high-load" sectors [63], to complement the existing LEP refrigerators, which have been upgraded in capacity and will feed the "low-load" sectors of the LHC. The adjudication rule took into consideration, besides capital investment, the integrated costs of operation over a period of ten years, thus giving a premium to efficiency, and – indirectly – compactness [64]. On the basis of the offers received two contracts were placed for the supply of two refrigerators each. Although based on different variants of the Claude cycle, both types of machines are designed to reach similar efficiencies, around 29 % with respect to the Carnot cycle [65, 66], corresponding to a coefficient-of-performance around 230 W per W. Based on three pressure cycles (typically 0.1-0.4-2 MPa), the refrigerators comprise a compressor station and a cold box. Each compressor station has five to eight oil-lubricated screw compressors, water refrigerant for helium and oil as well as a final oil removal system achieving an oil content of a fraction of ppm. The installed electrical input power is about 5 MW per refrigerator. The cold boxes are vacuum insulated and house the aluminium plate-fin heat exchangers and from eight to ten turbo-expanders to provide the cooling capacity. The built-in pre-cooler of 600 kW capacity, which is mainly provided by boiling-off liquid nitrogen is only used for the cool-down to 80 K [67]. Switchable 80 K absorbers remove up to 50 ppm of air and a 20 K adsorbed removes remaining traces of hydrogen and neon. In addition, switchable dryers are connected at the ambient temperature cold box inlet to remove humidity.

11.8.3 1.8 K Refrigeration Units

The efficient production of 1.8 K refrigeration in the multi-kW range [68, 69] – a novel requirement set by the LHC project – may only be achieved practically through combined cycles making use of sub-atmospheric cryogenic compressors and heat exchangers [70]. To foster the development of these technologies, CERN procured prototype low-pressure heat exchangers of different designs from industry as well as three hydrodynamic compressors, each handling 18 g s^{-1} at 1 kPa (10 mbar) suction pressure, with a pressure ratio of 3 all of which were evaluated by CEA, Grenoble (France), [71]. The thorough test campaigns performed on the latter have permitted the investigation of such critical issues as impeller and diffuser hydrodynamics, mechanical and thermal design, drive and bearing technology, as well as their impact on overall efficiency. Design and optimisation studies have also been performed in liaison with industry on refrigeration cycles matched to the expected performance of full-size machinery and meeting the requirements and boundary conditions of the project [72, 73]. This preparatory work permitted the launch of the procurement for the eight 1.8 K refrigeration units in 1998, through a successful call for tenders based on a functional and interface specification [74]. Two contracts have placed for the delivery and installation of four units each. The overall coefficient-of-performance of these 1.8 K refrigeration units, once attached to the main 4.5 K refrigerators of the LHC, is expected to be around 900 W per W [75, 76]. The first unit of each supplier has been tested [77].

Although being relatively simple, the cycle of these 1.8 K refrigeration units is somehow particular, as they have to be interconnected to 4.5 K refrigerators to allow production of cooling capacity at 1.8 K. A set of three or four centrifugal cold compressors delivers gas through heat exchangers to screw compressors, at a pressure between 30 and 50 kPa (300 and 500 mbar) to minimise the volumetric capacity of the latter. The cold compressors are equipped with active magnetic bearings operated at ambient temperature with rotational speeds from 200 to 800 Hz for the warmest stages. Isentropic efficiency of 75 % has been achieved reproducibly on several sets of cold compressors. As the return temperature to the 4.5 K refrigerator was imposed at 20 K, re-cooling after the heat exchangers with a turbo expander was necessary within the 1.8 K refrigeration units. The cooling capacity to be achieved defines the delivery pressure of the warm compressors (typically 0.3 to 0.6 MPa). Switchable 80 K absorbers are provided to remove up to 50 ppm of air as for other refrigerators.

11.9 INSTRUMENTATION

The cryogenic operation of the LHC requires a large number of sensors, electronic conditioning units and actuators, most of which are located inside the machine tunnel and must therefore withstand the radiation environment. This environment imposes strict radiation qualification procedures for the instrumentation located inside the tunnel. An inventory of the cryogenic instrumentation is shown in Tabs. 11.12 and Tab. 11.13 indicates the range and accuracy requirements for the whole data acquisition and processing chain. While a large number of sensors and actuators in this table are commercially available, specific tests on prototypes have been performed to select the suitable instrumentation. Furthermore all tunnel electronics are custom designed to be radiation tolerant.

The tight temperature margins allowed along the cryo-magnet strings require the implementation of precision cryogenic thermometry (overall measurement uncertainty down to ±10 mK, see Tab. 11.13) on an industrial scale (several thousand channels) with long-term robustness and reliability. Following the construction and commissioning of cryogenic calibration facilities of metrological class at CERN [78] and CNRS Orsay (France) [79], several types of sensors have been tested for performance in LHC environmental conditions on statistically significant ensembles. In particular, the effects of neutron irradiation at cryogenic temperature [80, 81] and of thermal cycling [82] have been investigated on several hundred thermometers, in order to select appropriate solutions for the project.

The stringent requirements on temperature measurements, once applied to signal conditioning, cannot be met by commercially available equipment. Several conditioner architectures, which could simultaneously provide the large dynamic range, accuracy, stability and tolerance to radiation levels as encountered in most of the LHC areas, have been investigated and prototyped in discrete component and ASIC versions [83].

During final helium filling and normal operation it is very important to know when the cryo-magnet cold-mass is completely filled with pressurised superfluid helium. This information is obtained from warm

pressure transducers hydraulically connected to the cold-mass enclosures via the instrumentation feedthroughs.

As a rule, instrumentation sensors used for control and that are not exchangeable without breaking the vacuum, are duplicated for redundancy. An exception is the cold mass temperature sensors, where redundancy is provided by the adjacent cold-mass temperature sensor.

Table 11.12: Cryogenic instrumentation inventory

Sensor type	Quantity	Redundancy	RadTol quantity
Temperature CX	4,500	1,153	3,347
Temperature Pt100	2,400		450
Pressure Low	230		230
Pressure Mod/High	900		900
Level Gauges	300		300
Electrical Heater	2,500		2,000

Table 11.13: Measurement uncertainty requirements versus temperature.

Temperature Range	1.6-2.2 K	2.2-4 K	4-6 K	6-25 K	20-300 K
Uncertainty [K]	± 0.01	± 0.02	± 0.03	± 1	± 5

11.10 PROCESS CONTROL

The process control system follows an industrial approach and is composed of Programmable Logic Controllers (PLCs) and a Supervisory Control and Data Acquisition (SCADA) systems. These are used in the operator interface and data logging system in three different layers based in a pyramidal organization.

The LHC cryogenic system uses equipment that is either localised in five geographical locations or distributed around the 27 km LHC tunnel. The corresponding control hardware architecture is different in order to save cabling costs and keep subsystems with a certain degree of autonomy. Local cryogenic equipment (e.g. refrigerators, interconnection boxes, storage, etc) has always been interfaced with industrial controllers and the solutions adopted are based in the previous experience with the LEP cryogenics.

However, the wide distribution of the cryogenics and the late availability of complete system require the development of off-line dynamic models and running them in simulation in order to start the machine operation in an optimal way.

The tunnel hardware is composed of standard industrial equipment and of distributed, radiation tolerant, Input/Output (I/O) units. The industrial equipment is installed in protected areas (16 alcoves and 8 IPs) and it is composed of PLCs, Ethernet gateways, fieldbus gateways, “intelligent” valve positioners and ancillary equipment. The distributed I/O units are custom designed to withstand the radiation in the arcs and the DS regions. Data exchange between PLCs and distributed I/O elements is performed via an industrial fieldbus [84].

Control algorithms have been designed, implemented and validated in the LHC test string and will be extended to simulate the LHC interconnected cell of a whole sector. The main control challenge is to regulate the LHC magnets temperature within the very tight margins in spite of it being a strongly non-linear process that exhibits a very large inverse response and a variable dead time [85]. The final choice of strategy, between absolute and relative temperature control, is not made and selection factors like the availability of the saturated pressure sensor or the change in the process dynamics are now under study. An expert tuning tool is required because of the impracticality of manually tuning all the closed control loops in the 216 LHC cells. LHC test string results showed the poor performance of the PID regulation when it is tuned too conservatively to avoid instabilities and demonstrated the improvement achieved by implementing advanced controllers.

11.11 CRYOGEN STORAGE AND MANAGEMENT

11.11.1 Helium

Helium inventory

Helium is mainly contained in the magnet cold masses which require a minimum filling ratio of 15 $l.m^{-1}$ of superfluid helium for enthalpy buffering (measured cold masses filling ratio is about 20 $l.m^{-1}$) and in the header C of the cryogenic distribution line. Header C requires a DN100 diameter for cool-down and warm-up operation and is filled with dense supercritical helium in normal operation. Fig. 11.16 shows the helium inventory per sector. The total helium inventory of the whole machine is about 96×10^3 kg. The complete storage of this inventory would cost about 20 MCHF for vessels and require a large implantation area. To limit costs and reduce the environmental impact, it was decided to provide gas storage for only half of the inventory.

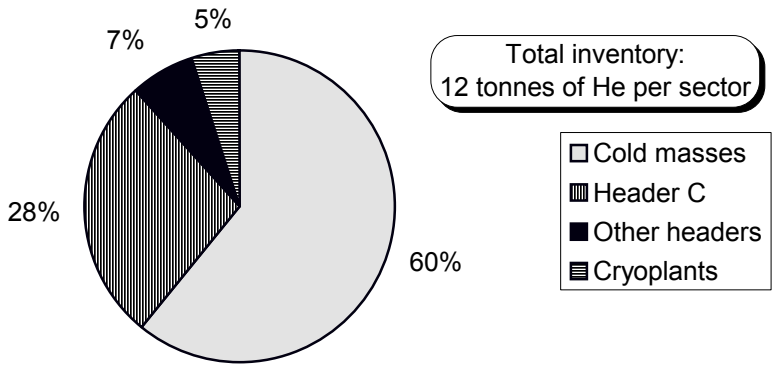

Figure 11.16: Helium inventory per sector

Gas storage management

The cryogenic system of LHC reuses the infrastructure recovered from LEP, which is composed of 40 vessels with a capacity of 75 m^3 each. These vessels with a diameter of 3 m and a height of 12 m have been installed in the shadow of the buildings. To complete this storage, additional vessels have been ordered in two steps in European industry. These additional vessels of 250 m^3 capacity each, a length of 28 m and a diameter of 3.5 m, are installed horizontally to limit their environmental impact. All vessels are in carbon steel. The gaseous helium is stored at a maximum working pressure of 2 MPa (20 bar) and ambient temperature. Fig. 11.17 shows the type and number of vessels distributed on the eight sites around the LHC ring [86].

At each point, four 250 m^3 vessels are used as buffer in case of resistive transition of multiple magnets during operation. These vessels must remain empty during normal operation and may only be used as storage capacity during shutdown. Helium at a temperature down to 10 K may be discharged into the buffer. In order to avoid cold spots on the carbon steel surface, the cold helium is diffused via a 26 m long stainless steel inlet pipe perforated with 41 holes that are 5 mm in diameter; this diffuser is connected to the buffer wall by means of a stainless steel cold finger. The lowest possible temperature of the buffer walls in case of resistive transition of a complete LHC sector is estimated to –35 °C.

The remaining vessels will be used as make-up gas storage for the cryogenic system. The filling of these vessels will be made with helium taken at the full flow dryer discharge, guaranteeing water and oil-free helium in the storage.

The storage vessels are not equally distributed reflecting the available space at the different points. The easy accessibility for helium delivery to some points like e.g. Point 1.8 is also taken into consideration. A helium line interconnecting the different storage areas will be installed in the tunnel and the access shafts. Each sector refrigerator is directly connected to its make-up storage. At Point 3 and 7, where no refrigerators

are installed, make-up storage vessels are also available. Make-up storage can be interconnected by opening the V1 valves.

In the case of resistive transition, helium leaves the cold environment via the interconnection box (QUI) and the return modules (QRLR) of the cryogenic distribution line; the buffers are filled via valves V2. The helium then returns to the sector refrigerator via valves V3 or V4. These are also used during a partial LHC warm-up to store one part of the inventory in the buffers. In this case, no electrical powering of the adjacent sectors is allowed. To minimise the dead volume in the buffers, it is also possible to finish their emptying by connecting them via the helium ring line and valves V5 to the low pressure (LP) of one refrigerator. The hydraulic impedance of the helium ring line (DN100 diameter pipe) does not diminish the liquefaction capacity of the refrigerator during re-cool-down of a sector.

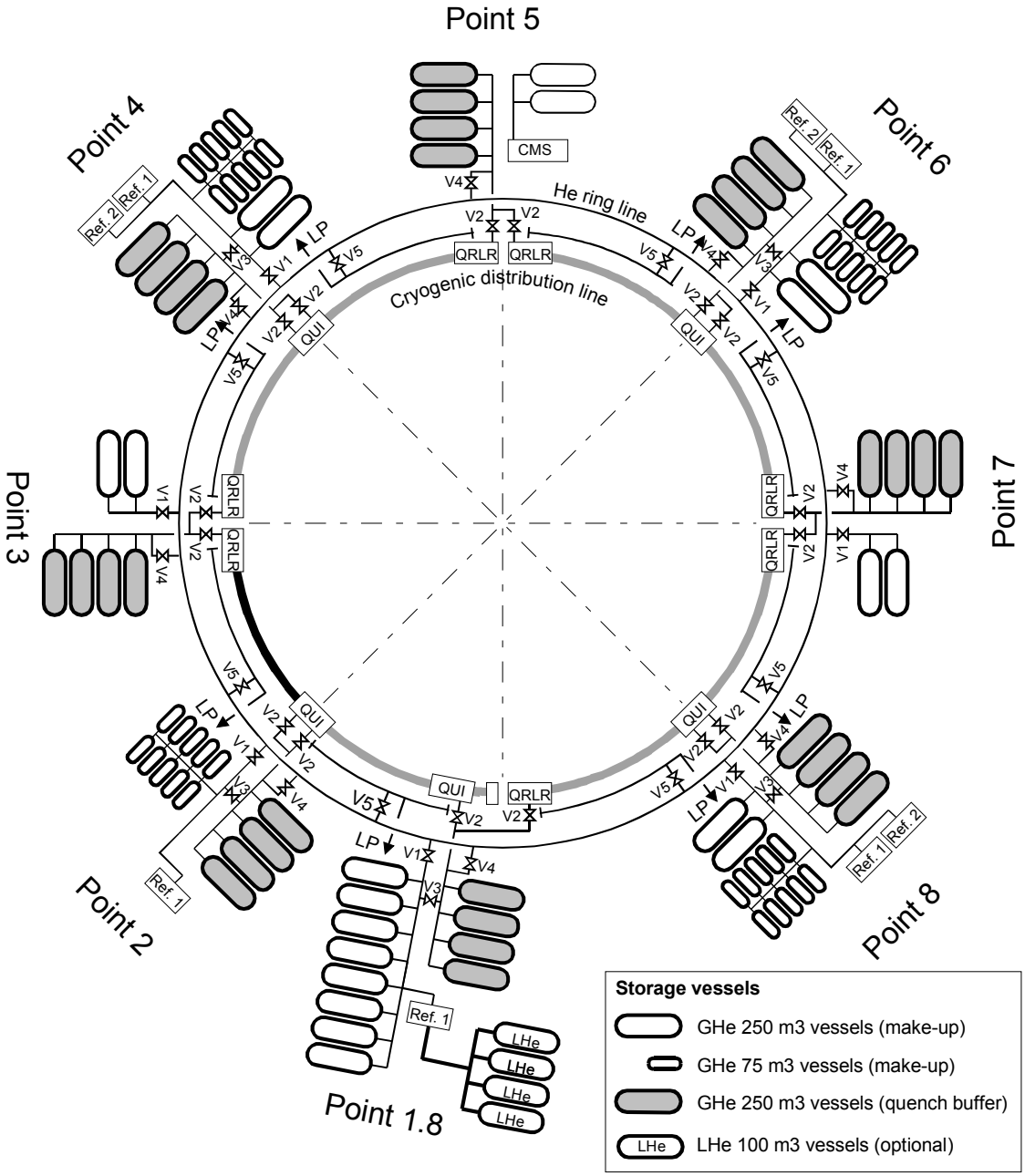

Figure 11.17: Helium storage management

"Virtual" or liquid storage

As the gas management allows storing only half of the inventory, during winter shutdown the excess (50 tonnes or about 400000 litres of liquid helium) has to be either "virtually" recovered by a gas distributor in the framework of an ad hoc contract ("virtual storage") or stored in liquid state in a central storage. Losing this helium to atmosphere, which corresponds to a cost of about 1.5 MCHF per shutdown, is economically not acceptable.

In the "virtual" storage contract, given notice, the company has to place at CERN's disposal standard 11000-gallon (about 40000 litres) industrial containers compatible with liquid helium handling by European distributors. Using the new 4.5 K refrigerators located at ground level, CERN will liquefy the exceeding inventory directly in the containers. During the shutdown period, the gas distributor will put the helium back on the market. During the re-cool-down phase following the shutdown, the distributor is committed to re-supply CERN with the same liquid amount. Studies are also under way about the possible contamination of the helium by activated solid particles or by transmutation of helium into tritium. The conclusion of these studies could impose that the helium inventory has to stay on the CERN site and consequently to immobilise the distributor containers for several months and preclude the "virtual" storage contract.

The best location of this central storage is at Point 1.8 in the vicinity of the new 4.5 K refrigerator in SD18. This central storage could comprise four 30000-gallon (about 110000 litres) containers for fixed storage. These containers with a diameter of 3.5 m and a length of 21 m have to be installed horizontally. The corresponding storage footprint of about 500 m^2 seems compatible with the impact study of Point 1.8. The loss rate of these containers is about 0.09 % per day, i.e. about 8 % per shutdown period. To avoid this loss, which corresponds to about 120 kCHF per shutdown, permanent re-liquefaction could be envisaged using a small liquefier (0.5 g s^{-1}). This storage option, which is under study, is not yet approved by the project management.

11.11.2 Liquid Nitrogen

Cooldown and purification

Nitrogen is only used for the cool-down operation and for regeneration of purifiers. For safety reasons, distribution of nitrogen in the LHC tunnel is forbidden. In addition, to avoid heavy operational logistics, permanent nitrogen consumption is avoided. In normal cool-down of a sector, the 600 kW pre-cooler will use a maximum liquid nitrogen flow-rate of 2.8 l s^{-1} and consume a total amount of liquid nitrogen of 1260 tonnes. Warm gaseous nitrogen is periodically used to regenerate dryer and absorber beds. Tab. 11.14 gives the corresponding flow-rate consumption and the duration of the cool-down and regeneration operations. Liquid nitrogen is also used in some type of refrigerators to regenerate absorbers, but the quantities are negligible on this scale.

Table 11.14: Liquid nitrogen requirements

Operation	Maximum LN2 flow rate [l s^{-1}]	Operation duration [h]	Expected frequency [operation/year]	Total per operation [ton]
Sector cool-down	2.8	200	1	1260
Dryer regeneration	0.36	50	8	324

Logistics

At each of the five cryogenic islands, two liquid nitrogen reservoirs having a unit storage capacity of 50000 l are installed close to the SD refrigerator buildings. For the purpose of producing gaseous nitrogen, an atmospheric heater is coupled to the liquid nitrogen reservoir. In the case of a parallel cool-down of the LHC sectors, the liquid nitrogen consumption would correspond to about 50 full liquid nitrogen standard containers per day, i.e. one container delivery every 2 hours (day and night) at a cryogenic island with two refrigeration plants. The logistics concerning the liquid nitrogen delivery is essential for a continuous cool-down operation. The two reservoirs will be filled alternately in less than one hour to match the volume

required. To relax this logistics constraint, the machine cool-down could be staged by operating some sectors in series. During the winter shutdown, if no intervention on the installation requiring circuit opening is needed, the sector can stay cold floating, thus reducing the re-cool-down time and simplifying the liquid nitrogen logistics.

REFERENCES

[1] L. Evans, LHC Accelerator Physics and Technology Challenges, PAC'99, New York (1999).
[2] Ph. Lebrun, The Large Hadron Collider, A Megascience Project, CERN-LHC-Project-Report-374.- Geneva, 5 Apr 2000.
[3] The LHC study group, Design study of the Large Hadron Collider (LHC), CERN Report 91-03 (1991).
[4] Ph. Lebrun, Advanced Superconducting Technology for Global Science : The Large Hadron Collider at CERN, CERN-LHC-Project-Report-499.- Geneva, 27 Aug 2001.
[5] The LHC study group, The Large Hadron Collider Accelerator Project, eds. Y. Baconnier, G. Brianti, Ph. Lebrun, A. Mathewson and R. Perin, CERN/AC/93-03 (LHC) Report (1993).
[6] The LHC study group, The Large Hadron Collider, Conceptual Design, eds. P. Lefèvre and T. Pettersson, CERN/AC/95-05 (LHC) Report (1995).
[7] Ph. Lebrun, Superconductivity and Cryogenics for the Large Hadron Collider, CERN- LHC-Project-Report-441.- Geneva, 27 Oct 2000.
[8] Ph. Lebrun, Superfluid helium cryogenics for the Large Hadron Collider project at CERN, Proc. ICEC15 Genova, Rizzuto and Federghini editors, Butterworth-Heinemann (1994) pp. 1-8
[9] G. Bon Mardion, G. Claudet and P. Seyfert, Practical Data on Steady-State Heat Transport in Superfluid Helium at Atmospheric Pressure, Cryogenics, Vol. 19 (1979) 45-47.
[10] Ph. Lebrun, Advances in Cryogenics at the Large Hadron Collider, ICEC17, Bournemouth (1998).
[11] Ph. Lebrun, Cryogenics for the Large Hadron Collider, IEEE Trans. Appl. Superconductivity 10 1 (2000) pp. 1500-1506
[12] S. Claudet et al., Four 12 kW / 4.5 K Cryoplants at CERN, Cryogenics 34 ICEC Supplement (1994) 99-102.
[13] M. Chorowski et al, A Simplified Cryogenic Distribution Scheme for the Large Hadron Collider, Adv. Cryo. Eng. 43A (1998) 395-402.
[14] A. Ballarino, A. Ijspeert and U. Wagner, Potential of High Temperature Superconductor Current Leads for LHC Cryogenics, Proc. ICEC16, Elsevier Science, Oxford, UK (1997) 1139-1142.
[15] J.C. Brunet et al., Design of the Second-Series of LHC Prototype Dipole Magnet Cryostats, Adv. Cryo. Eng. 43A (1998) 435-441.
[16] W. Erdt, G. Riddone and R. Trant, The Cryogenic Distribution Line for the LHC: Functional Specification and Conceptual Design, CEC'99 Montreal (1999).
[17] M. Mathieu et al., Supporting Systems from 293 K to 1.9 K for the LHC Cryomagnets, Adv. Cryo. Eng. 43A (1998) 427-434.
[18] G. Ferlin et al., Comparison of Floating and Thermalised Multilayer Insulation Systems at Low Boundary Temperature, Proc. ICEC16, Elsevier Science, Oxford, UK (1997) 443-446.
[19] D. Camacho et al, Heat Inleak Measurements on LHC Components, CEC'99 Montreal (1999).
[20] G. Riddone, Analisi teorica e Verifica Sperimentale delle Prestazioni Termiche dei Criostati Prototipi del Progetto LHC, Doctoral thesis, Politecnico di Torino, Italy (1997).
[21] V. Benda et al., Measurement and Analysis of Thermal Performance of LHC Prototype Cryostats, Adv. Cryo. Eng. 41A (1996) 785-792.
[22] O. Grobner, The LHC Vacuum System, Proc. PAC'97 3, IEEE Piscataway, NJ, USA (1998) 3542-3546.
[23] E. Hatchadourian, Ph. Lebrun and L. Tavian, Supercritical Helium Cooling of the LHC Beam Screens, Proc. ICEC17, IoP, Bristol, UK (1998) 793-796.
[24] R. Saban et al, First Results and Status of the LHC Test String 2, CERN-LHC-Project-Report-568.- Geneva, 02 Jul 2002.
[25] E. Blanco et al., The Cryogenic System for the LHC Test String 2: Design, Commissioning and Operation, CERN-LHC-Project-Report-614.- Geneva, 15 Nov 2002.

[26] E. Hatchadourian, Stability and Control of Supercritical Helium Flow in the LHC Circuits, CEC'99 Montreal (1999).
[27] J.B. Bergot et al., Thermal Performance of the LHC Short Straight Section Cryostat, CERN-LHC-Project-Report-571, 02 Jul 2002.
[28] L. Dufay, C. Policella, J.M. Rieubland and G. Vandoni, A Large-scale Test Facility for Heat Load Measurements down to 1.9 K, CERN-LHC-Project-Report-510, 19 Oct 2001.
[29] M. Chorowski, P. Grzegory, C. Parente and G. Riddone, Experimental and Mathematical Analysis of Multilayer Insulation below 80 K, CERN- LHC-Project-Report-385, 26 Jul 2000.
[30] M. Chorowski, P. Grzegory, C. Parente and G. Riddone, Optimisation of Multilayer Insulation : an engineering approach, CERN-LHC-LHC-Project-Report-464, 12 Feb 2001.
[31] J. Livran et al., A Cryogenic Test Set-Up for the Qualification of Pre-Series Test Cells for the LHC Cryogenic Distribution Line, CERN-LHC-Project-Report-380, 26 Jul 2000.
[32] G. Riddone, D. Rybkowski and R. Trant, Results from the Qualification of the three Pre-series Test Cells for the LHC Cryogenic Distribution Line, CERN-LHC-Project-Report-610, 15 Nov 2002.
[33] A. Ballarino et al., A Low Heat Inleak Cryogenic Station for Testing HTS Current Leads for the Large Hadron Collider, CEC'99 Montreal (1999).
[34] Ph. Lebrun, Superfluid helium as a Technical Coolant, Atti XV Congresso Nazionale sulla Trasmissione del Calore, Edizioni ETS, Politecnico di Torino, Italy (1997) 61-77.
[35] Ph. Lebrun, L. Serio, L. Tavian and R. van Weelderen, Cooling Strings of Superconducting Devices below 2 K: The Helium II Bayonet Heat Exchanger, Adv. Cryo. Eng. 43A (1998) 419-426.
[36] J. Casas et al., Design Concept and First Experimental Validation of the Superfluid Helium System for the Large Hadron Collider, Cryogenics 32 ICEC Supplement (1992) 118-121.
[37] A. Gauthier et al., Thermohydraulic Behaviour of He II in Stratified Co-current Two-phase Flow, Proc. ICEC16, Elsevier Science, Oxford, UK (1997) 519-522.
[38] B. Rousset et al., Thermohydraulic Behaviour of HeII in Stratified Co-Current Two-Phase Flow at High Vapor Velocities, CERN-LHC-Project-Report-617, 15 Nov 2002.
[39] E. Di Muoio et al., Optical Investigations of HeII Two Phase Flow, CERN-LHC-Project-Report-516, 19 Oct 2001.
[40] D. Camacho et al., Thermal characterisation of the LHC HeII heat exchanger tube, Proc. ICEC17, IoP, Bristol, UK (1998) 647-650.
[41] J. Casas-Cubillos et al., Operation, Testing and Long-Term Behaviour of the LHC Test String Cryogenic System, Proc. ICEC17, IoP, Bristol, UK (1998) 747-750.
[42] B. Flemsaeter et al., Applying Advanced Control Techniques for the Temperature Regulation of the LHC Superconducting Magnets, Proc. ICEC17, IoP, Bristol, UK (1998) 631-634.
[43] E. Blanco-Viñuela, J. Casas-Cubillos and C. de Prada-Moraga, Linear Model-Based Predictive Control of the LHC 1.8 K Cryogenic Loop, CEC'99 Montreal (1999).
[44] E. Blanco et al., He II Heat Exchanger Test Unit for the LHC Inner Triplet, CERN-LHC-Project-Report-505, 19 Oct 2001 (Published in: AIP Conf. Proc.: 613 (2002) no. 1, pp.147-154).
[45] R. Byrns et al., The Cryogenics for the LHC Interaction Region Final Focus Superconducting Magnets, Proc. ICEC17 Bournemouth, Dew-Hughes, Scurlock and Watson editors, IoP (1998) pp. 743-746
[46] A. Ballarino, HTS Current Leads for the LHC Magnet Powering System, CERN-LHC-Project-Report-608, 15 Oct 2002.
[47] L. Liu, G. Riddone and L. Tavian, Update of a Cooldown and Warmup Study for the Large Hadron Collider, CERN-LHC-Project-Report-507, 19 Oct 2001.
[48] L. Liu, G. Riddone and L. Tavian, Refined Studies of Cooldown and Warmup for the Large Hadron Collider, CERN-LHC-LHC-Project-Report-618, 15 Nov 2002.
[49] M. Chorowski, Ph. Lebrun, L. Serio and R. van Weelderen, Thermohydraulics of Quenches and Helium Recovery in the LHC Prototype Magnet Strings, Cryogenics 38 (1998) 533-543.
[50] M. Chorowski, P. Grzegory, L. Serio, and R. van Weelderen, Modelling of Helium-mediated Quench Propagation in the LHC Prototype Test String-1, CERN- LHC-Project-Report-468, 23 Mar 2001.
[51] M. Chorowski and B. Skoczen, Thermo-Mechanical Analysis of Cold Helium Injection into Gas Storage Tanks Made of Carbon Steel Following Resistive Transitions of the LHC Magnets, Proc. ICEC17, IoP, Bristol, UK (1998) 755-758.

[52] L. Dufay, A. Perin and R. van Weelderen, Characterisation of Prototype Superfluid Helium Safety Relief Valves for the LHC Magnets, CEC'99 Montreal (1999).
[53] A. Bézaguet et al., A Facility for Accurate Heat Load and Mass Leak Measurements on Superfluid Helium Valves, CEC'99 Montreal (1999).
[54] M. Chorowski, Ph. Lebrun and G. Riddone, Preliminary Risk Analysis of the LHC Cryogenic System, CEC'99 Montreal (1999).
[55] M. Chorowski, G. Konopka and G. Riddone, Helium Discharge and Dispersion In the LHC Accelerator Tunnel in Case of Cryogenic Failure, CERN-LHC-Project-Report-381, 26 Jul 2000.
[56] M. Chorowski, W.K. Erdt, G. Konopka and G. Riddone, Oxygen Deficiency Hazard (ODH) Monitoring System in the LHC Tunnel, CERN-LHC-Project-Report-523, 13 Dec 2001.
[57] M. Chorowski, G. Konopka and G. Riddone, An Experimental Study of Cold Helium Dispersion in Air, CERN-LHC-Project-Report-508, 19 Oct 2001.
[58] M. Chorowski, G. Konopka, G. Riddone and D. Rybkowski, Experimental Simulation of Helium Discharge into the LHC Tunnel, CERN-LHC-Project-Report-611, 15 Nov 2002.
[59] H. Grünhagen, H. Posselt, J. Weber and H. Ahlers, Long, Bellows-Free Vertical Helium Transfer Lines for the LHC Cryogenic System, CERN-LHC-Project-Report-615, 15 Nov 2002.
[60] G. Riddone and R. Trant, The Compound Cryogenic Distribution Line for the LHC : Status and Prospects, CERN-LHC-Project-Report-612, 15 Nov 2002.
[61] Ph. Lebrun, G. Riddone, L. Tavian and U. Wagner, Demands in Refrigeration Capacity for the Large Hadron Collider, Proc. ICEC16, Elsevier Science, Oxford, UK (1997) 95-98.
[62] M. Barranco-Luque et al., Conclusions from Procuring, Installing and Commissioning Six Large-Scale Helium Refrigerators at CERN, Adv. Cryo. Eng. 41A (1996) 761-768.
[63] S. Claudet, Ph. Gayet and U. Wagner, Specification of Four New Large 4.5 K Refrigerators for the LHC, CEC'99 Montreal (1999).
[64] S. Claudet, Ph. Gayet, Ph. Lebrun, L. Tavian and U. Wagner, Economics of Large Helium Cryogenic Systems: Experience from Recent Projects at CERN, CEC'99 Montreal (1999).
[65] P. Dauguet, G.M. Gistau-Baguer and P. Briend, Two Large 18 kW (equivalent power at 4.5 K) Helium Refrigerators for CERN's LHC Project, Supplied by Air Liquide, CEC'99 Montreal (1999).
[66] J. Bösel, B. Chromec and A. Meier, Two Large 18 kW (equivalent power at 4.5 K) Helium Refrigerators for CERN's LHC Project, Supplied by Linde Kryotechnik AG, CEC'99 Montreal (1999).
[67] U. Wagner, Solutions for Liquid Nitrogen Pre-Cooling in Helium Refrigeration Cycles, CERN-LHC-Project-Report-387, 27 Jun 2000.
[68] Ph. Lebrun, L. Tavian and G. Claudet, Development of Large-Capacity Refrigeration at 1.8 K for the Large Hadron Collider, Proc. Kryogenika'96, Icaris, Praha, Czech Republic (1996) 54-59.
[69] L. Tavian, Large Cryogenics Systems at 1.8 K, CERN-LHC-Project-Report-412, 23 Sep 2000.
[70] P. Roussel, B. Jäger and L. Tavian, A Cryogenic Test Station for Subcooling Helium Heat Exchangers for LHC, CERN-LHC-LHC-Project-Report-386, 26 Jul 2000.
[71] A. Bézaguet, Ph. Lebrun and L. Tavian, Performance Assessment of Industrial Prototype Cryogenic Helium Compressors for the Large Hadron Collider, Proc. ICEC17, IoP, Bristol, UK (1998) 145-148.
[72] F. Millet, P. Roussel, L. Tavian and U. Wagner, A possible 1.8 K refrigeration Cycle for the Large Hadron Collider, Adv. Cryo. Eng. 43A (1998) 387-393.
[73] S. Claudet, Ph. Lebrun and L. Tavian, Towards Cost-To-Performance Optimisation of Large Superfluid Helium Refrigeration Systems, CERN-LHC-LHC-Project-Report-391, 27 Jun 2000.
[74] S. Claudet et al., Specification of Eight 2400 W at 1.8 K Refrigeration Units for the LHC, CERN-LHC-Project-Report-392, 26 Jul 2000.
[75] Hilbert, B., Gistau-Baguer, G. and Dagut, F., 2.4 kW at 1.8 K Refrigeration Units for CERN LHC Project Supplied by Air Liquide, ICEC18 Mumbaï 2000, India.
[76] H. Asakura et al., Four 2400 W / 1.8 K Refrigeration Units for CERN-LHC: the IHI/Linde System, ICEC18 Mumbaï 2000, India.
[77] S. Claudet et al., A Cryogenic Test Station for the Pre-series 2400 W at 1.8 K Refrigeration Units for the LHC, CERN-LHC-Project-Report-616, 15 Nov 2002.
[78] C. Balle, J. Casas and J.P. Thermeau, Cryogenic Calibration Facility at CERN, Adv. Cryo. Eng. 43A (1998) 741-748.
[79] E. Chanzy et al., Cryogenic Thermometer Calibration System using a Helium Cooling Loop and a Temperature Controller, Proc. ICEC17, IoP, Bristol, UK (1998) 751-754.

[80] J.F. Amand, J. Casas-Cubillos, T. Junquera and J.P. Thermeau, Neutron irradiation Tests in Superfluid Helium of LHC Cryogenic Thermometers, Proc. ICEC17, IoP, Bristol, UK (1998) 727-730.
[81] J. Casas-Cubillos et al., SEU Tests Performed on the Digital Communication System for LHC Cryogenic Instrumentation, CERN-LHC-LHC-Project-Report-503, 17 Oct 2001 (Published in Nucl. Instrum. Methods Phys. Res.).
[82] Ch. Balle et al., Influence of Thermal Cycling on Cryogenic Thermometers, CEC'99 Montreal (1999).
[83] J. Casas et al., Signal Conditioning for Cryogenic Thermometry in the LHC, CEC'99 Montreal (1999).
[84] T. Bager et al., Instrumentation, Field Network And Process Automation for the LHC Cryogenic Line Tests, CERN-LHC-Project-Report-395, 26 Jul 2000.
[85] E. Blanco-Viñuela, J. Casas-Cubillos, C. De Prada-Moraga and S. Cristea, Non-Linear Advanced Control of the LHC Inner Triplet Heat Exchanger Test Unit, CERN-LHC-Project-Report-506, 19 Oct 2001 (Published in: AIP Conf. Proc.: 613 (2002) no. 1, pp.1597-1604).
[86] M. Barranco-Luque and L. Tavian, Gaseous Helium Storage and Management in the Cryogenic System for the LHC, CERN-LHC-Project-Report-383, 26 Jul 2000.